Electron paramagnetic resonance and related phenomena in high-temperature superconductors

A. A. Romanyukha, Yu. N. Shvachko, and V. V. Ustinov

Institute of Metal Physics, Ural Branch of the Academy of Sciences of the USSR, Sverdlovsk
(Submitted March 19, 1991; resubmitted after revision June 20, 1991)
Usp. Fiz. Nauk **161**, 37–78 (October 1991)

An analysis is made of the results of EPR experiments in superconducting and nonsuperconducting samples of $YBa_2Cu_3O_{7-\delta}$, including samples irradiated by neutrons and samples with various admixed impurities. It is shown that the observed resonance signal in superconducting samples is due to impurity phases and that the diversity of detected signals from oxygen-deficient samples is probably due to polymorphism in the distribution of oxygen atoms. The results of investigations of the so-called low-field signal, which is due to the presence of a network of Josephson weak links, are discussed in detail for both ceramics and single crystals. The findings of EPR studies in high-temperature superconductors are summarized, and possible directions for further experiments are discussed.

1. INTRODUCTION

Although there have been many review articles published on various aspects of high-temperature superconductivity (see, e.g., Refs. 1–6), they have given practically no discussion of topics pertaining to electron paramagnetic resonance (EPR) in high-temperature superconducting compounds.

EPR has been used to study superconductors since the 1970s (see the reviews[7-9] and the literature cited therein). Most of the work at that time was done on intermetallic superconductors (e.g., $LaRu_2$, CeRu, LaEr, $LaAl_2$, etc.) containing a magnetic rare-earth ion (most often Gd, Er, or Eu) as a spin probe, which under certain conditions made it possible to observe an EPR signal. Those experiments yielded important information about the dependence of the superconducting transition temperature on the concentration of magnetic impurities and made it possible to measure the energy gap, to estimate the interaction integrals of the electronic subsystems with one other and with the lattice, and so forth.[7-9] However, the total number of studies of this nature is relatively small, comprising only something over 30 papers in almost 20 years of research. The main reason for this modest production, we believe, is the difficulty of making EPR observations in metals and intermetallides, since the strong exchange interaction of the magnetic moments of the rare-earth ions with one other and with the conduction electrons often causes a critical broadening of the EPR signal, making it impossible to observe. Moreover, it is not always possible to introduce a magnetic ion into an intermetallide lattice.

After the discovery of high-temperature superconductivity in 1986 there was an abrupt increase in the number of papers on EPR in superconductors, and by now there have been over 100 of them. The results show that the parameters of the EPR signal in high-temperature superconductors exhibit substantial differences in behavior from those of the superconductors investigated previously. Moreover, the high-temperature superconducting materials display a number of new effects that previously were not encountered or were insufficiently studied in intermetallic superconductors. Such effects include the so-called low-field signal, the low-field oscillations of the microwave absorption, and hysteresis effects in the microwave absorption.

The purpose of this review is to analyze the present status of EPR research on high-temperature superconductors and the prospects for further development of this field of study.

We begin by analyzing the pertinent properties of $YBa_2Cu_3O_{7-\delta}$ (Sec. 2). Next we discuss the results of EPR studies in high-temperature superconductors, concentrating on Y–Ba–Cu–O compounds (Sec. 3). We then examine the data on the low-field signal (Sec. 4), discuss the hysteresis of the microwave absorption (Sec. 5), and summarize the findings and discuss possible directions for development of EPR research on high-temperature superconducting materials (Sec. 6).

2. SOME PHYSICAL PROPERTIES OF Y–Ba–Cu–O

A particular aspect of the EPR method (and, incidentally, of other magnetic resonance methods) is that the experimental results must be processed with the use of some physical model, which presupposes preliminary knowledge of the basic structural, magnetic, and electrical properties of the sample. Figure 1 shows the structure of $YBa_2Cu_3O_7$ and the notation that we will be using for the atoms (the figure was taken from Ref. 10). The copper atoms in this structure have two inequivalent positions, denoted Cu1 and Cu2. Cu1 is located in a "chain" with oxygen O4 and has a valence of 2 + . It has been shown in a number of studies (see, e.g., Ref. 10) that the interaction between the magnetic moments of Cu1 is of a ferromagnetic nature. Cu2, the so-called "planar" copper, lies at the center of a rhombus, at the corners of which are oxygen atoms O2 and O3. The interaction between Cu2 atoms is antiferromagnetic.[11] The presence of distinct planes in the $YBa_2Cu_3O_7$ structure leads to an appreciable planar anisotropy in the properties of this compound; for example, the ratio of the second critical fields for magnetic field perpendicular and parallel to the plane of the sample is equal to six.[12] The stoichiometric composition $YBa_2Cu_3O_7$ has orthorhombic symmetry with $a = 3.823$ Å, $b = 3.884$ Å, $c = 11.670$ Å at 300 K. The data on the temperature dependence of the static magnetic susceptibility of

 0038-5670/91/100862-21$01.00

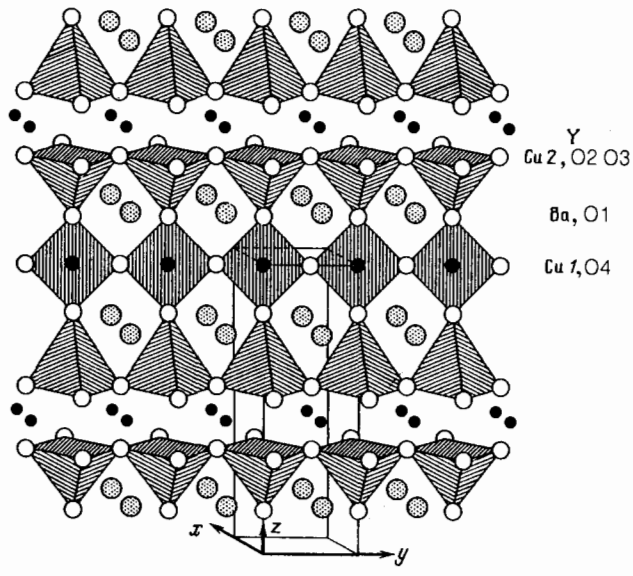

FIG. 1. Structure of $YBa_2Cu_3O_7$ (Ref. 10).

$YBa_2Cu_3O_{7-\delta}$ are rather inconsistent, but most authors consider the magnetic susceptibility of the stoichiometric phase to be practically independent of temperature at $T > T_c$ (Fig. 2). It has been reliably established that the conductivity of this compound is hole-type, but the data on the absolute value of the conductivity at room temperature fluctuate in different studies over three orders of magnitude around $10^{-3}\ \Omega\cdot$cm.[13] The properties of all high-temperature superconductors depend critically on their oxygen content.[14-21] Decreasing the oxygen content leads to a gradual degradation of the superconducting properties (Fig. 3), to a transition from an orthorhombic to a tetragonal structure, to the acquisition of insulating properties, and to a Curie–Weiss temperature dependence of the static magnetic susceptibility (see Fig. 2). Finally, $YBa_2Cu_3O_6$ exhibits antiferromagnetism with $T_N = 400$–500 K.[22-31]

The uniformity of the oxygen distribution over the sample in Y–Ba–Cu–O compounds depends strongly on the synthesis conditions.[6,10] Numerous studies of the surface of oxide superconductors (see, e.g., Refs. 32–34) have revealed the presence of an oxygen-deficient subsurface layer. This leads to the formation of semiconducting and insulating layers at the boundaries of superconducting grains in ceramic samples or at twin boundaries in single crystals. Since the skin depth at the microwave frequencies ordinarily used in EPR studies is about 10 μm at room temperature, this multiphasedness of the samples must have an effect on the measurements. Moreover, because of it the microwave properties can be influenced by the Josephson effect and by the dependence of the properties of the sample on the time that has passed since it was synthesized. Under these complicated experimental conditions it is important to develop selection and reliability criteria for the results of measurements.

3. EPR IN OXIDE SUPERCONDUCTORS

Observation of electron paramagnetic resonance requires the presence of magnetic moments in the material under study. Various experimental situations are possible in this regard: 1) the magnetic moments (both localized and those due to the current carriers) can exist in the investigated material itself; 2) magnetic impurities can be introduced for this purpose; 3) localized moments can be created in the sample by irradiating it with particles of some kind. Let us discuss the results obtained in these three kinds of experiments.

3.1. EPR on localized moments in oxide superconductors

Most of the experiments have been done on $YBa_2Cu_3O_{7-\delta}$ (Refs. 35–57) and $GdBa_2Cu_3O_{7-\delta}$ (Refs.

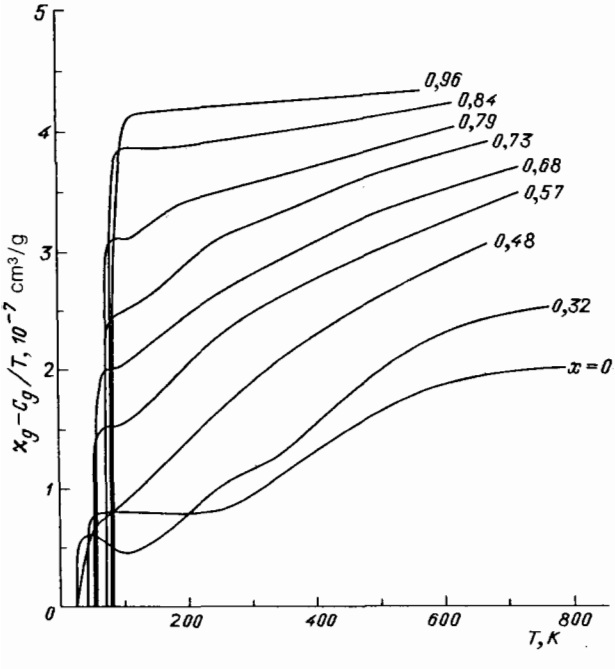

FIG. 2. Temperature dependence of the static magnetic susceptibility without the Curie-like contribution from the impurities (C_g/T) in $YBa_2Cu_3O_{6+x}$ for various oxygen concentrations (Ref. 19).

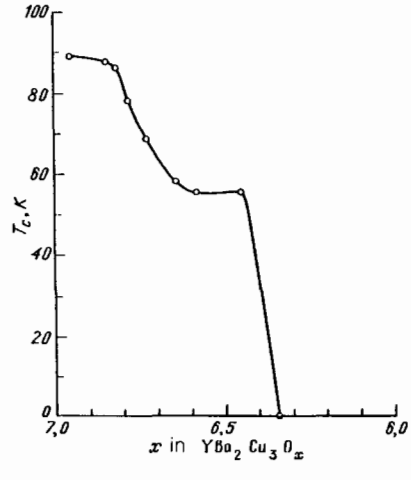

FIG. 3. Dependence of the superconducting transition temperature T_c on the oxygen concentration x in $YBa_2Cu_3O_x$ (Ref. 10).

37, 49, 55, 58–62), although other compounds have also been studied.[63–65] The published data on EPR in oxide superconductors are extremely contradictory. Many authors[35–42] have reported the observation of EPR in superconducting samples of $YBa_2Cu_3O_7$. Others[43–57] have found it absent in this compound or have attributed the signal to some impurity phase. More than half of the authors have attributed the observed EPR signal to Cu^{2+}. However, there are other interpretations: for example, in Ref. 36 it is attributed to oxygen, while in Ref. 49 the signal observed there was thought to be a superposition of signals from the Cu1, Cu2 and O^- moments.

Various circumstances can come into play in the correct assessment of the experimental results for superconducting samples. Since $YBa_2Cu_3O_{7-\delta}$ and other oxide superconductors have an appreciable conductivity at room temperature, the shape of the resonance line can be influenced by the skin effect. As was first shown by Dyson,[66] the resonance line will have an appreciable asymmetry in this case, and its shape will be described by the expression

$$P = \frac{\omega H_1^2}{4}(\delta A)\omega_0\chi_0 T_2 \cdot \frac{1}{2}\frac{1 - T_2(\omega - \omega_0)}{1 + T_2^2(\omega - \omega_0)^2}, \qquad (3.1)$$

where P is the power absorbed by the sample at resonance, χ_0 is the susceptibility of the subsystem of localized moments, ω is the microwave frequency, δ is the skin depth, T_2 is the spin–spin relaxation time, ω_0 is the resonance frequency, and A is the surface area of the sample.

For EPR of localized moments in a conductor the ratio of the maximum to the minimum of the first derivative of the power absorbed at resonance should be about 3, and the asymmetry of the resonance signal should vary with temperature and with grain size in a definite way, according to Eq. (3.1). Moreover, as the temperature decreases, the linewidth in a conducting sample should generally vary according to the relation

$$\Delta H_{1/2} = a + b(T - \vartheta), \qquad (3.2)$$

here ϑ is the paramagnetic Curie temperature, and b is the Korringa slope of the linewidth:

$$b = \pi k_B [J_{sf}\rho(E_f)]^2/g\mu_B, \qquad (3.3)$$

where k_B is Boltzmann's constant, μ_B is the Bohr magneton, J_{sf} is the exchange interaction integral of the localized moments with the conduction electrons, and $\rho(E_F)$ is the density of states at the Fermi level. It follows, in particular, that the residual EPR linewidth should be close to the linewidth ΔH of the signal from Cu^{2+} in insulators.

It has been shown by EPR studies in superconducting intermetallides[7–9] that the transition to the superconducting state is accompanied by a sharp change in the g factor, in the linewidth, and in the intensity of the line, which is proportional to the spin susceptibility. After transition to the superconducting state the shape of the resonance signal changes and is described by an expression different from Eq. (3.1).[8]

If we examine the published results of EPR studies in high-temperature superconductors from the standpoint of the ideas presented above, we can find no case that exhibits even a majority of the indicated attributes. The observed signal most likely corresponds to the $d_{x^2-y^2}$ term of Cu^{2+}.

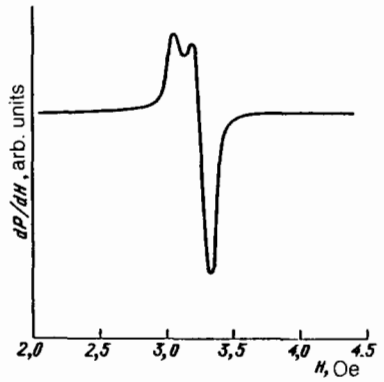

FIG. 4. Shape of the EPR signal from impurities in a ceramic sample of $YBa_2Cu_3O_{7-\delta}$.

The shape of the detected signal (Fig. 4) usually corresponds to the case of an anisotropic g factor, which is most typical of compounds with low electrical conductivity. The temperature dependence of the width of the detected signal displays a remarkable diversity: in Refs. 35, 38, and 39 the spectra are said to be temperature independent, whereas in Refs. 36, 41, and 42 a strong temperature dependence of the linewidth is reported for samples of about the same composition. In a number of studies the signal observed in superconducting samples is attributed to the so-called "green" phase of Y_2BaCuO_5, as was rather convincingly demonstrated by a comparison of the EPR measurements on samples prepared by different technologies. However, the value of the EPR parameters and their temperature dependences in superconducting samples differ substantially from the data for the "green" phase. The key to understanding these differences apparently lies in the features of the electronic properties of the insulating and superconducting phases that exist at the surface of the superconducting grains. There is an interesting possibility of using the localized moments in these phases as a probe for studying the superconducting properties.[49] Certain peculiarities of the experiments in which EPR was detected in superconducting samples also argue in favor of an impurity origin of the signal in them. For example, in Refs. 35 and 49 the samples in which the signal was observed were reported to have a significant width of the superconducting transition, and in Ref. 36 only freshly prepared samples were used.

Thus EPR in superconducting samples is most likely due to nonsuperconducting impurity phases. The absence of a resonance signal from the magnetic moments of Cu^{2+} in the superconducting phases is evidently due to the strong broadening of the EPR line as a result of their strong exchange interaction with one another and with holes. This interpretation is also supported by the fact that conduction in oxide superconductors goes via the "copper" planes and chains. The most common impurity phases in $YBa_2Cu_3O_7$ are the oxygen-deficient phases $YBa_2Cu_3O_{7-\delta}$, Y_2BaCuO_5 (Refs. 43–45, 51, 67), $Y_2Cu_2O_5$ (Ref. 68), and several others.

3.2. EPR in oxygen-deficient samples of $YBa_2Cu_3O_{7-\delta}$

Varying the oxygen content in $YBa_2Cu_3O_{7-\delta}$ leads to a significant change in the physical properties. When the

oxygen concentration in $YBa_2Cu_3O_{7-\delta}$ is changed from 7 to 6, one observes the following: there is a structural transition, the superconducting transition temperature exhibits two plateaus near 90 K and 60 K (see Fig. 3), the superconductivity vanishes, and antiferromagnetism appears. For $0.6 < \delta < 1$ neutron diffraction experiments[69,70] reveal a continuous change in T_N from 0 to 400 K. These extremely interesting properties make these compounds attractive objects for study by the EPR method, which is sensitive to structural and, especially, local magnetic phase transitions.[49,57,71,72] However, the results of these studies are contradictory, which is not surprising, since often the results of other experiments on oxygen-deficient samples of $YBa_2Cu_3O_x$ do not correlate with each other either (see, e.g., Refs. 29 and 73–76). This situation is apparently due to the fact that for intermediate oxygen concentrations there exist several possible metastable microscopic distributions of oxygen. In other words, two samples with the same oxygen content can be substantially different in terms of the presence or absence of microscopic ordering, which causes the observed structure parameters and electronic behaviors to be different. The usual procedure for preparing oxygen-deficient samples is to heat a $YBa_2Cu_3O_7$ sample to a temperature of 500–900 °C, at which this compound loses oxygen, and then quenching it to room temperature. However, rapid quenching leads to a "freezing in" of the high-temperature equilibrium microscopic state of the oxygen sublattice, and as a result the properties of $YBa_2Cu_3O_{7-\delta}$ compounds with the same oxygen content have a wide spectrum of properties, depending strongly on the annealing temperature. Therefore, oxygen-deficient samples must be carefully characterized by methods (e.g., neutron and x-ray diffraction, magnetic susceptibility) which are sensitive to the structural and magnetic characteristics. Moreover, in this situation it is particularly important to start with single-phase samples of $YBa_2Cu_3O_7$ for the oxygen-depletion annealing. As we have said, EPR is one of the most sensitive methods for checking whether a sample is single-phase. In Ref. 57, where the indicated conditions were fulfilled, a resonance signal was observed for $T < 50$ K in $YBa_2Cu_3O_{6.28}$, $YBa_2Cu_3O_{6.15}$, and $YBa_2Cu_3O_{6.10}$ samples.

Figure 5 shows the temperature dependence of the parameters of the EPR signal for these samples. One of the interesting results here is the observation of a fractional power-law dependence of the integrated intensity of the EPR signal on temperature: $\chi_s \sim T^{-\alpha}$, with $\alpha = 0.71$, 0.82, and 0.95 for $\delta = 0.72$, 0.85, and 0.90. Such a dependence had been observed previously in studies of quasi-one-dimensional compounds.[77,78] Moreover, since the magnetic moments in the $Cu(2)^{2+}$ position are coupled by a strong exchange interaction, which should strongly broaden the EPR signal, it can be concluded[11,57] that the observed signal is due to $Cu(1)^{2+}$. This result agrees with the conclusions of Ref. 10, where it was found by electron microscopy that the decrease in the oxygen content in $YBa_2Cu_3O_7$ occurs only in the O4 position, i.e., in the Cu–O chains.

In this interpretation the fractional power-law dependence of the spin susceptibility χ_s can be due to a singularity in

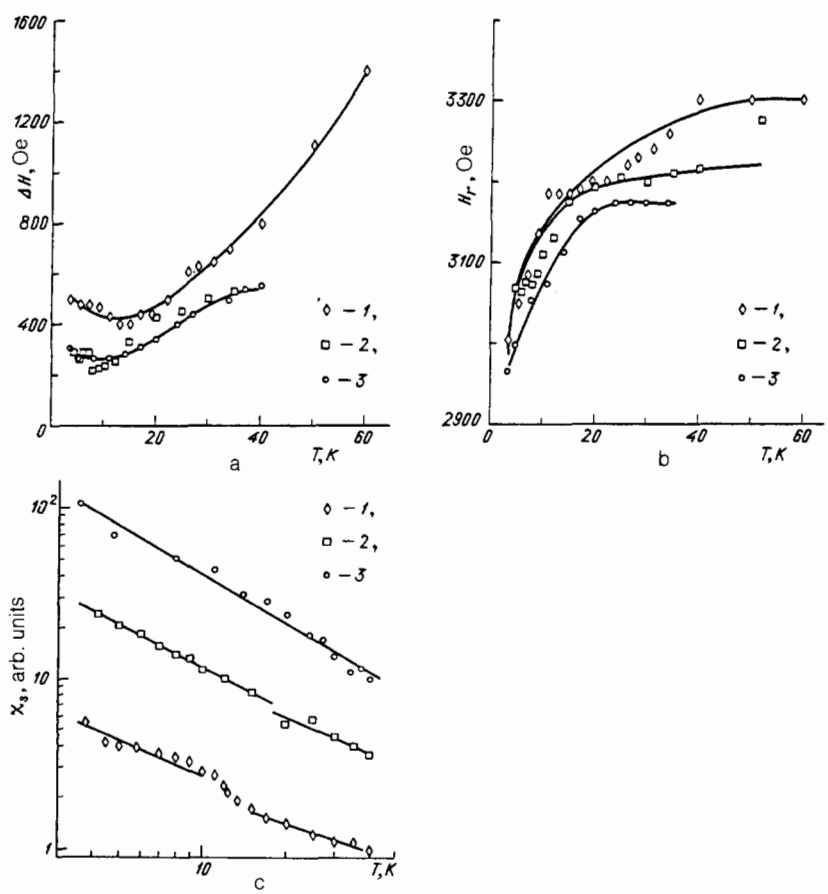

FIG. 5. Temperature dependence of the parameters of the EPR signal for oxygen-deficient nonsuperconducting samples of $YBa_2Cu_3O_{7-\delta}$ (Ref. 57). *1*) $\delta = 0.72$; *2*) $\delta = 0.85$; *3*) $\delta = 0.9$. a) Temperature dependence of the EPR linewidth ΔH for $YBa_2Cu_3O_{7-\delta}$. b) Temperature dependence of the resonance field H_r for $YBa_2Cu_3O_{7-\delta}$. c) Temperature dependence of the relative spin susceptibility χ_s for $YBa_2Cu_3O_{7-\delta}$.

the distribution of the exchange interaction at $J \to 0$, i.e., $P(J) \sim J^{-\alpha}$. In this case an estimate gives

$$\chi_s(T \to 0) \sim \int \frac{dJP(J)}{T + \text{const} \cdot J} \sim T^{-\alpha}. \tag{3.4}$$

Assuming that the magnetic moments are distributed around one (and only one) vacancy, we easily find that

$$P(J) = p(L) \left| \frac{dL}{dJ} \right|, \tag{3.5}$$

where L is the length of the whole Cu–O–Cu–O fragment between vacancies. If we assume a Poisson distribution

$$p(L) = L_0^{-1} \exp(-L/L_0), \quad L_0 = a/\delta, \tag{3.6}$$

(a is the distance between magnetic moments in the chain) and a dependence of the form

$$J(L) = J_0 \exp(-L/d), \tag{3.7}$$

we obtain

$$\alpha = 1 - (d/L_0) = 1 - (d\delta/a). \tag{3.8}$$

This expression agrees satisfactorily with the experimental results.

We see from Fig. 5a that $\Delta H(T)$ has three characteristic intervals. At relatively high temperatures ΔH decreases with decreasing T, then it passes through a minimum in the region 10 K $< T <$ 15 K, and for $T <$ 10 K it increases. A comparison of these data with the temperature dependence of H_r and χ_s shows that magnetic phase transitions occur at 10 K $< T <$ 15 K, at least for compounds with $\delta = 0.77$ and 0.85; this conclusion agrees with the neutron data,[69,10] which indicate the presence of transitions to an antiferromagnetic state.

In view of the impurity character of the resonance signal from superconducting samples, the observed[10] diversity of metastable microscopic arrangements of the oxygen in the Cu–O chains on deoxygenation can account for the contradictory nature of the EPR results for both superconducting and nonsuperconducting compositions $YBa_2Cu_3O_{7-\delta}$. This casts doubt on the correctness of using the technique of determining the oxygen content in YBaCuO from the change in the lattice parameters or by thermogravimetry.

The conclusive EPR experiments on oxygen-deficient samples are apparently yet to be done, since it is important to investigate the different phase of $YBa_2Cu_3O_{7-\delta}$ with the annealing and quenching conditions varied in a controlled way and to elucidate the relationship of EPR to the superconducting and magnetic properties of these compounds.

3.3. Study of high-temperature superconducting materials by EPR with added impurities

As we have said, the magnetic and superconducting properties of high-temperature superconductors can be investigated by EPR of the localized magnetic moments of impurities admixed into the composition $YBa_2Cu_3O_{7-\delta}$ to serve as a probe. Among the various ions used for this purpose, Gd^{3+} is prominant for several reasons. It has spin $S = 7/2$ and therefore ordinarily gives an anisotropic EPR spectrum with seven lines, due to the allowed transitions $\Delta M = \pm 1$. The Hamiltonian in this case can be written in the form[80]

$$H = g\mu_B SH + \sum_{k,l} B_k^l O_k^l, \tag{3.9}$$

where B_k^l are the crystalline-field parameters, and the summation is over k and l. One can use (3.9) to calculate the angular dependence of the EPR resonance field and to determine the B_k^l. Naturally, the observed spectrum is very sensitive to the interaction between the Gd^{3+} spin and other magnetic subsystems present in the compound. In particular, this interaction can induce mutual spin-flip transitions, which lead to exchange narrowing of the EPR line. This effect has been studied repeatedly in intermetallides and is satisfactorily described by the Barnes–Plefka theory.[9]

Experiments on $Gd_xY_{1-x}Ba_2Cu_3O_{7-\delta}$ have been reported in many papers (see, e.g., Refs. 49, 59–61, 72, 80, 81). Measurements have been made on both ceramic and single-crystal samples. The EPR spectrum, as in superconducting intermetallides, consists of 7 lines (Fig. 6), whose positions in single crystals and in oriented samples depend on the angle between the magnetic field direction and the plane of the sample. One of the interesting results obtained in this system is the high degree of similarity of the EPR spectra and spectral parameters in superconducting and insulating samples. Both kinds of samples exhibit exchange narrowing due to the interaction between Gd^{3+} and Cu^{2+}, which can be described in the framework of the Barnes–Plefka approach. In Ref. 80 the crystalline-field parameters were calculated from the experimental data. Although the intensity of the EPR signal from Gd^{3+} in the superconducting samples was considerably weaker than in the insulating samples, the shape of the resonance line in the superconducting samples for $T > T_c$

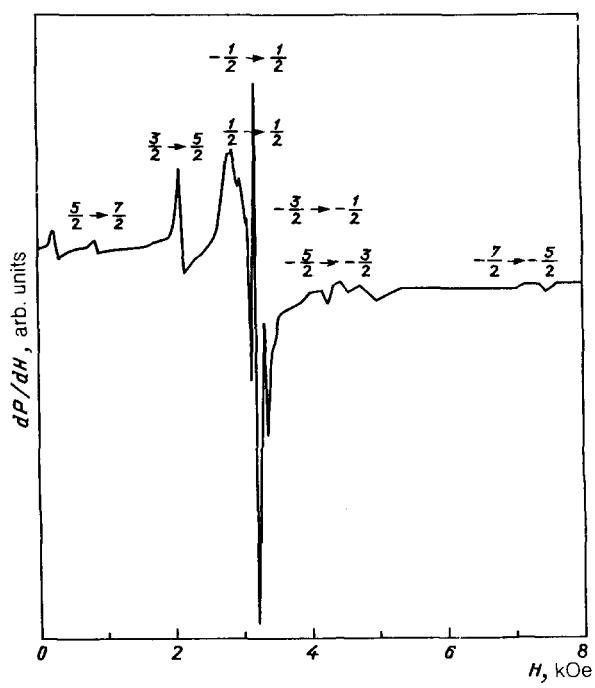

FIG. 6. Shape of the EPR spectrum for nonsuperconducting $Gd_xY_{1-x}Ba_2Cu_3O_{7-\delta}$ (Ref. 72).

differed strongly from the Dyson form (3.1).[80] The similarity of the EPR parameters for insulating and superconducting samples may be due to the relatively weak interaction of the magnetic moments of Gd^{3+} with the conduction electrons in the latter. This interpretation is supported by the extremely small changes in the superconducting properties of the Y–Ba–Cu–O system when Y is replaced by other rare-earth elements.[1-5] Hence it is understandable why the shape of the EPR spectrum from Gd^{3+} in superconductors near T_c remains nearly constant.[59,60,80] For this reason one cannot extract the parameters of the superconducting state from measurements on $Gd_xY_{1-x}Ba_2Cu_3O_{7-\delta}$, as has been done for intermetallides.[8,9] The same result has been obtained[49,82-85] by the admixture of a small amount of Hf, Eu, or Ho in Y–Ba–Cu–O, but, unlike the case of the $Gd_xY_{1-x}Ba_2Cu_3O_{7-\delta}$ system, here the EPR signal is either not observed or is detected from the insulating or semiconducting phases. A rather unexpected result was obtained in a study[86] of the effect of doping with Er and Yb, where EPR signals with g factors characteristic of the ions Er^{3+} ($g = 4.2$–6.8) and Yb^{3+} ($g = 3.2$–0.2) were detected in superconducting samples of $Y_{0.99}Er_{0.01}Ba_2Cu_3O_{7-\delta}$ and $Y_{0.99}Yb_{0.01}Ba_2Cu_3O_{7-\delta}$, respectively. At the point of the superconducting transition the nature of the temperature dependence of both the linewidth and amplitude of the EPR signal from these ions changed. This is somewhat strange, since even the complete replacement of yttrium by erbium or ytterbium has only an insignificant effect on T_c.[87] The nature of the vanishing of the resonance signals after the deoxygenating annealing of superconducting samples is also puzzling, especially when the results of Ref. 87 are compared with those obtained by doping with gadolinium.

Since the replacement of Ba in YBaCuO by Sr or Ca also has little effect on the superconducting properties, it is of great interest to study the effects of replacement of the copper. In an EPR study[64] of superconducting compounds $EuBa_2(Cu_{1-y}M_y)_3O_{9-\delta}$ (where M = Cr, Mn, Fe, Co, Ni, Zn) it was found that the replacement of copper led to a significant decrease in T_c, e.g., in the case $y = 0.05$, by $\Delta T_c = 70$ K for M = Zn, by $\Delta T_c = 47$ K for M = Co, by $\Delta T_c = 42$ K for M = Fe, and by $\Delta T_c = 27$ K for M = Ni ($T_c = 92$ K for the initial composition $EuBa_2Cu_3O_{9-\delta}$). In itself the sharp decrease in T_c on replacement of Cu by Zn is rather surprising, since Zn has the configuration $3d^{10}$ and is nonmagnetic. The observed signal was attributed by the authors to an impurity phase; the temperature dependence of its EPR parameters is extremely close to that observed for superconducting samples of $YBa_2Cu_3O_{7-\delta}$ (see Fig. 5 in Sec. 3.2). For the superconducting phases no EPR signal was observed in $EuBa_2(Cu_{1-y}M_7)_3O_{9-\delta}$. A more interesting result was obtained in an EPR study[88] of $La_{1.82}Sr_{0.18}(Cu_{1-x}Zn_x)O_4$. In the absence of Zn no signal was observed in this high-temperature superconductor. Upon doping with zinc an EPR signal could be observed starting at 0.5 at.% Zn. It is important to note that the samples used in Ref. 88 (unlike Ref. 64) were oriented in a magnetic field, and no EPR signal was observed in unoriented samples because of the large anisotropy. On the basis of the experimental data on the shift of the g factor, its angular dependence, and the temperature dependence of the static susceptibility, it was concluded that the localized moments are located on the copper, which forms a complex with zinc.

There have been a number of EPR studies of $YBa_2(Cu_{1-x}Fe_x)O_{7-\delta}$, in which the copper is partially replaced by iron.[57,89] Here again in the superconducting compositions no EPR signal was observed, possibly for the same reason as for superconducting samples without iron (see paragraph 3.1). An important result found here by EPR studies of nonsuperconducting samples is that the magnetic properties of Y–Ba–Cu–O change significantly when even a small amount of iron is added. This circumstance necessitates a more critical appraisal of the results of Mössbauer studies of oxide superconductors.

3.4. The effect of irradiation on the EPR properties of $YBa_2Cu_3O_{7-\delta}$

The effect of irradiation on the superconducting properties of $YBa_2Cu_3O_{7-\delta}$ has been investigated in a number of studies,[30,57,90-92] in which radiation defects were produced by irradiation with γ rays, electrons, neutrons, and ions. A general result of these studies is the suppression of superconductivity as the irradiation dose increases. This effect is apparently due to damage to the Cu–O bonds both in the planes and in the chains in YBaCuO. Irradiation also leads to a partial redistribution of the oxygen atoms in the O4 and O5 positions and to an appreciable increase in the lattice parameters a, b, and c. With increasing fluence $\Phi > 1\cdot 10^{19}$ cm^{-2} the superconductivity vanishes; the linear temperature dependence $\rho(T)$ goes over to a dependence of the Mott type, $\rho(T) \sim \exp(T_0/T)^{1/4}$. The EPR method has been used to investigate irradiated samples in two studies.[57,92] In Ref. 57 neutrons were used for the disordering. Observation of the signal was possible only for nonsuperconducting samples of $YBa_2Cu_3O_{6.8}$ with a maximum fluence of $\Phi = 2\cdot 10^{19}$ cm^{-2}. The form of this signal and the values of its parameters were close to those observed in oxygen-deficient samples (see Sec. 3.2). Since magnetic susceptibility measurements[30] show that even small doses ($\Phi \sim 10^{18}$ cm^{-2}) increase the susceptibility and lead to a Curie–Weiss temperature dependence, it can be supposed that the magnetic moments giving the EPR signal are found in Cu–O chains, while the localized moments formed at low doses of irradiation are mainly in the planes (i.e., in the Cu2 position). The strong antiferromagnetic interaction between the magnetic moments at Cu2 causes a large broadening of the signal, so that it becomes impossible to observe.

Figure 7 shows the experimental results of EPR studies of an irradiated sample ($\Phi = 2\cdot 10^{19}$ cm^{-2}). We notice here that the linewidth and resonance field are independent of temperature, that the phase transition to an antiferromagnetic state which is observed for oxygen-deficient samples does not occur here, and that the spin susceptibility has a temperature dependence of the specific form $\chi_s \sim T^{-0.5}$. This last fact may mean that for $\Phi = 2\cdot 10^{19}$ cm^{-2} the localization at Cu1 is rather weak.

In Ref. 92 the EPR method was used to study a $YBa_2Cu_3O_{7-\delta}$ sample ($T_c = 95$ K) that had been uniformly intermixed with the radioactive α emitter $^{239}PuO_2$. As time went on (i.e., as the dose increased) the superconductivity of the sample was gradually suppressed, and two EPR signals appeared: one from Cu^{2+}, of the same nature as that described above, and another, more intense, which the authors attributed to radiation defects of the type O_2^-.

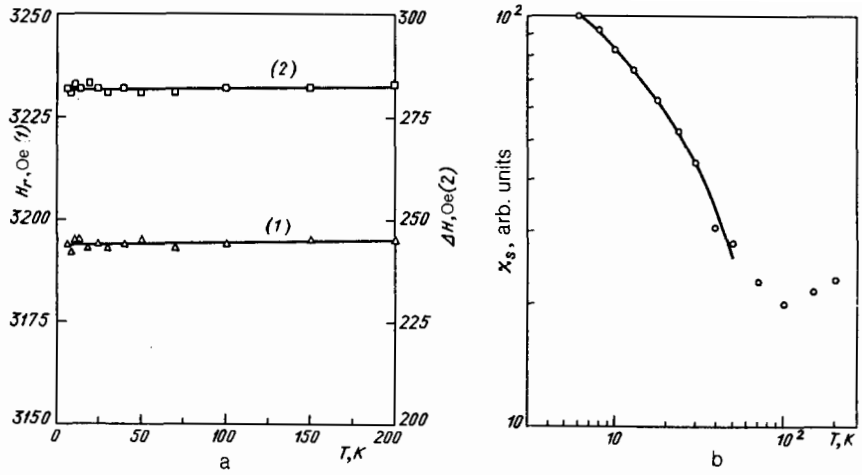

FIG. 7. a) Temperature dependence of the EPR linewidth ΔH (right-hand scale) and resonance field (left-hand scale) in neutron-irradiated $YBa_2Cu_3O_{6.78}$; $\Phi = 2\cdot 10^{19}$ cm^{-2} (Ref. 57). b) Temperature dependence of the relative spin susceptibility χ_s in neutron-irradiated $YBa_2Cu_3O_{6.78}$; $\Phi = 2\cdot 10^{19}$ cm^{-2}. The continuous curve is a logarithmic fit (Ref. 57).

3.5. Use of EPR to defect the distribution of vortices in high-temperature superconductors

A new method for investigating the distribution of vortices by using the EPR signal from localized moments deposited on the surface of a superconductor has recently been proposed.[93,94] The idea behind this technique is the same as in experiments on the inhomogeneous broadening of an NMR line on transition to the vortex-current state.[95] The coating used was the organic compound diphenyl picryl hydrazyl (DPPH), which is widely used in EPR as a sensitivity standard and as a benchmark for determining the g factor. The EPR linewidth in DPPH is quite narrow (a few oersteds) and is weakly dependent on temperature. Figure 8 shows the temperature dependence of the EPR linewidths for a DPPH powder and for DPPH adsorbed on the ceramic superconductor $YBa_2Cu_3O_7$. One can clearly see the inhomogeneous broadening of the resonance signal due to the onset of vortices. According to Ref. 95, the second moment of the field distribution in the superconductor is given by the expression

$$\overline{\Delta H_s^2} = \frac{\Phi_0^2}{16\pi^3\lambda^4}, \tag{3.10}$$

where Φ_0 is the flux quantum and λ is the penetration depth of the field. If the second moment of the EPR line observed in the normal state is denoted ΔH_n^2, the resultant width of the signal below T_c will be given by the expression

$$\Delta H_{pp} = 2(\overline{\Delta H_n^2} + \overline{\Delta H_s^2})^{1/2}. \tag{3.11}$$

The component ΔH_n^2 is due to the spin interactions of the DPPH radicals on the surface and does not change at the transition to the superconducting state. From expressions (3.10) and (3.11) one can determine the penetration depth of the field into the superconductor,

$$\lambda(T) = \frac{\lambda_0}{[1-(T/T_c)^4]^{1/2}}, \tag{3.12}$$

where λ_0 is the penetration depth at $T = 0$ K. Figure 9 shows the temperature dependence $\lambda(T)$ calculated in Ref. 94 in comparison with the BCS theory. The dependence is in satisfactory agreement with the data obtained from experiments on μ^+SR[96] and NMR.[97]

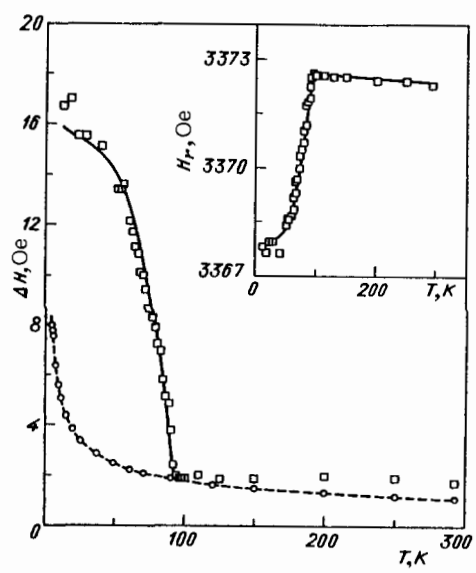

FIG. 8. Temperature dependence of the EPR linewidth for a DPPH powder and for DPPH adsorbed on the surface of a ceramic $YBa_2Cu_3O_{7-\delta}$ superconductor. The inset shows the temperature dependence of the resonance field for DPPH on $YBa_2Cu_3O_{7-\delta}$ (Ref. 94).

3.6. EPR of twins and superconducting single crystals of $YBa_2Cu_3O_{7-\delta}$

Crystals of oxide superconductors are highly subject to twinning. In Ref. 98 the structure of twins in YBaCuO single crystals was investigated by EPR and a classification of twins was given. In the normal state three EPR lines, which depended on the orientation of the crystal in the magnetic field, were observed, and for $H \parallel c$ these signals coalesced into one, whose width varied in the interval 330–130 Oe as the temperature was lowered from 300 K to 100 K. Near the superconducting transition ($T_c = 90$ K) the signal broadened sharply, so that it became impossible to observe. A classification of defects can be done on the basis of the orientation dependence of the g factors of the three observed signals (Fig. 10). This dependence is indicative of the existence of

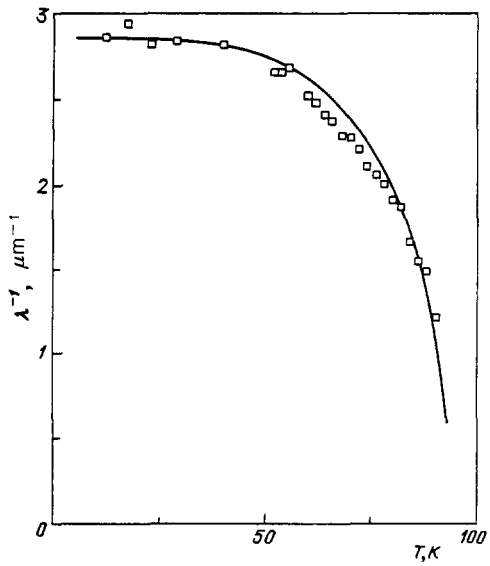

FIG. 9. Temperature dependence of the penetration depth λ of the magnetic field into a superconductor, as calculated from the EPR data of Ref. 94 (see Fig. 8).

three types of paramagnetic complexes, *A*, *B*, and *C*, which differ in the nature of the environment of the Cu^{2+} ion. Since, as we have said, the EPR signal can be observed only from the chain copper Cu1, one can draw qualitative conclusions as to the structure of these complexes from the orientation dependence of the *g* factors. Figure 11 shows the structures of the observed twin complexes obtained in Ref. 98 from the EPR data.

4. LOW-FIELD SIGNAL IN HIGH-TEMPERATURE SUPERCONDUCTING CERAMICS

4.1. Main experimental results

A characteristic feature of all the EPR spectra for ceramic high-temperature superconducting samples in the su-

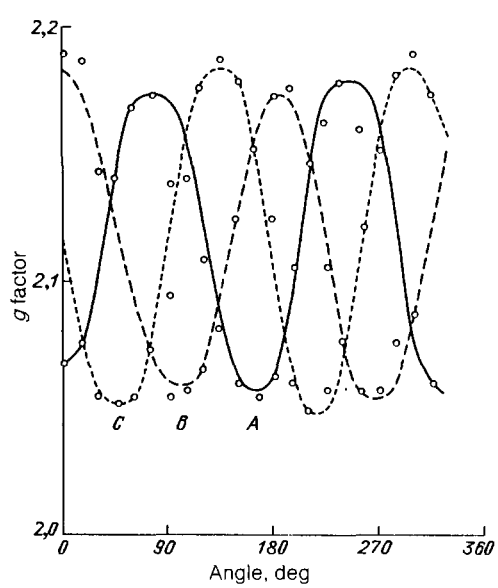

FIG. 10. Orientation dependence of the *g* factor of the three EPR lines for three types of defects in a YBaCuO single crystal (Ref. 98).

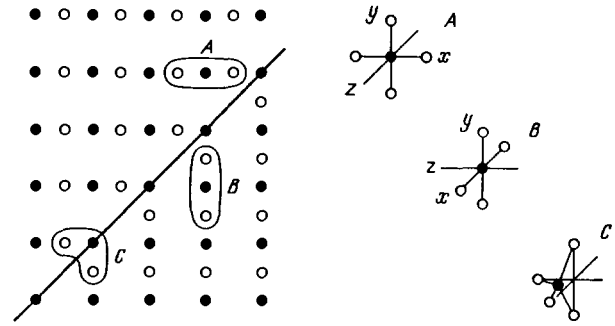

FIG. 11. Structure of the observed twin complexes in a YBaCuO single crystal, as inferred from the EPR data of Ref. 98.

perconducting state is the existence of an intense signal near zero field, whose phase is inverted relative to that of the absorption signal.[99-107] The nature of this signal, the temperature dependence of its parameters, and the susceptibility turn out to be different for ceramics of the same composition prepared by different technologies. For example, when the average size of the granules is decreased from 50 to 10 μm in a $YBa_2Cu_3O_7$ powder, the value of the magnetic field at which saturation of the absorption occurs changes from $H = 16$ Oe to 40 Oe at $T = 77$ K, and the absolute value of the absorbed power in these fields, $P(H)$, changes from $0.10P_n$ to $0.06P_n$, where P_n is the microwave power absorbed by the sample in the normal state.[128]

Analysis of the published data shows that the temperature dependence of the integrated intensity of the low-field signal, $I(T)$, also depends on the quality of the sample. For example, in multiphase $YBa_2Cu_3O_{7-\delta}$ ceramics exhibiting a semiconductor-like growth of the electrical conductivity at low temperatures and an intense impurity EPR signal at $T < T_c$ one observes a monotonic growth in the intensity $I(T)$ of the low-field signal all the way down to helium temperatures. In contrast, for multiphase samples with a metallic behavior of the conductivity and a wide transition (75–91 K) the growth of $I(T)$ saturates at low temperatures, and the low-field signal arises for $T < 91$ K. Finally, in stoichiometric compositions $YBa_2Cu_3O_{6.9}$ with a narrow transition and a metallic behavior of the conductivity the intensity of the low-field signal exhibits a maximum at temperatures approaching T_c and declines monotonically with increasing perfection of the sample [$T_c - T_{max} \geqslant 5$ K] and with further decrease in temperature. The pertinent data are shown in Fig. 12. The nature of the decline $I_{max}/I(20\text{ K}) = 5 - 10$, which is substantially different for samples of similar quality, correlates with the density of the ceramic under study.[43,116] However, compaction of an yttrium ceramic by a pressure of 4 GPa with shear fundamentally alters the nature of the low-field signal.[123] An "additional" EPR signal arises at zero field for $T < T_c$, with the usual phase for an absorption signal. The intensity of the new signal increases monotonically with decreasing temperature, and at $T < 85$ K it completely suppresses the low-field signal. It should be noted that the appearance of an "additional" signal in high-temperature superconducting ceramic materials without the application of an external pressure has been reported in a

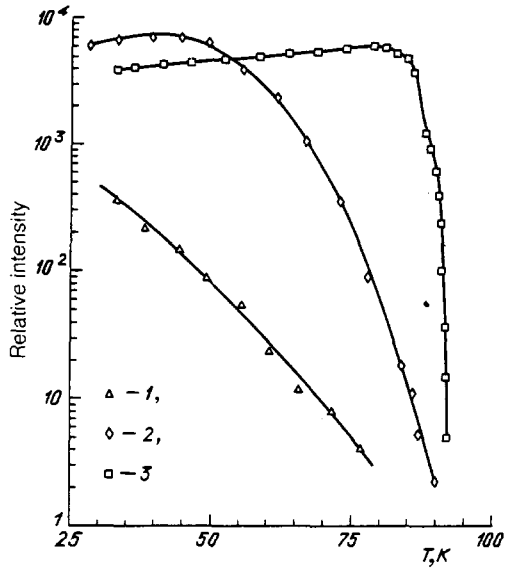

FIG. 12. Temperature dependences of the intensity of the low-field signal for $YBa_2Cu_3O_{7-\delta}$ ceramics prepared by different technologies (Ref. 116): *1*) for samples having a semiconductor-like behavior of the electrical conductivity at $T > T_c$, $\rho(200\ \mathrm{K}) = 13\ \Omega$; *2,3*) for samples having a linear behavior of the conductivity, with different widths of the superconducting transition ΔT (points *2* correspond to a multiphase ceramic with $\Delta T \approx 15$ K, points *3* to a single-phase ceramic with $\Delta T \approx 1$ K, $\rho(T \to T_c) = 8\ \mathrm{m}\Omega$). The curves joining the experimental points are the result of a spline interpolation.

number of papers,[100,106] but in these cases the signal was weaker.

An interesting experimental fact is the presence of hysteresis in the microwave absorption in zero field. The value of the corresponding "coercive" field G has been found[128] to depend on temperature and the microwave frequency ω. For example, for an yttrium ceramic G rose from 6 Oe to 50 Oe when the sample was cooled from 14 to 3.8 K. Increasing the microwave frequency from 22 to 35 GHz also led to a 5-fold increase in G. Measurements of the magnetization $M(H)$ in this interval of fields did not reveal any hysteretic anomalies. Moreover, it follows from the published data that the value of the low-field hysteresis is also sensitive to low-frequency modulation of the microwave power.

The original result was obtained by smoothly varying the amplitude of the scanning magnetic field H_{sc}.[128,112–115] At a fixed temperature and a low scanning amplitude $H_{sc} \leqslant H^*$ ($H^* = 25$ Oe, 4.2 K, 35 GHz; Ref. 128) no low-field absorption was detected. On further increase in the scanning amplitude, $H_{sc} > H^*$, a low-field signal appears, shifted by the amount of the hysteresis.

Detailed investigations of the low-field signal under conditions such that low-field hysteresis exists reveal a pronounced time dependence. The difference in the intensities of the low-field signal during the forward ($I_\uparrow$) and backward ($I_\downarrow$) field scans, $\Delta I = (I_\uparrow - I_\downarrow)$, relaxes exponentially toward a fixed (under external conditions) value ΔI_0 that depends linearly on the "coercive" field G. For example, for yttrium ceramics $(I_\uparrow - I_\downarrow)/I_\uparrow$ falls off from 7.3 to 5.2 over a time of 140 sec, whereas for $Tl_{0.5}Pb_{0.5}Sr_2CaCu_2O_7$ it falls from 1.0 to 0.66 over the same amount of time.[126] This behavior is a direct indication that nonlinear and relaxation effects play an important role in the formation of the low-field signal.

The class of objects exhibiting a low-field signal is not limited to high-temperature superconducting ceramics. Low-field absorption has by now been detected in a number of conventional type-II superconductors prepared in the form of fine powders and composites.[32] Thus analysis of the published results on the low-field signal in various ceramic high-temperature superconducting systems supports the assertion that its qualitative behavior is independent of the chemical composition and that it is a consequence of the granular structure of the samples.

4.2. Model of the low-field signal in ceramics

A basic property of granular superconductors is the existence of intergranular Josephson weak links. From this standpoint a ceramic superconductor can be regarded as a network of Josephson links threading through a bulk superconductor.

Under the conditions of an EPR experiment the following currents circulate on the surface of the superconductor: I_0, the current that screens the static external magnetic field (the scanning field H_{sc}); $I_{mw}\cos(\omega_{mw}t)$, the current caused by the incidence of the microwave field on the sample; and I_M, the current caused by the low-frequency modulating field H_M. Treating these currents (in the zero-modulation approximation) as transport currents, for an isolated intergranular weak link on the surface of the sample one can write an equation for the phase shift $\phi = \phi_0 + \phi_{mw}$ in the space between two granules:

$$\frac{Ch}{2e}\frac{d^2\phi}{dt^2} + \frac{1}{R}\frac{\hbar}{2e}\frac{d\phi}{dt} + I_c\sin\phi = I_0 + I_{mw}\cos(\omega_{mw}t), \tag{4.1}$$

where R, C, and I_c are the normal resistance, the capacitance, and the critical current of the link. In the low-field approximation ($I_0 < I_c$) and neglecting the capacitance of the contact, Eq. (4.1) admits an approximate analytical solution (the equation is linearized with respect to ϕ_{mw}) for the absorbed microwave power P:

$$P = P_n\frac{1}{1+\eta}\left(P_n = \frac{1}{2}I_{mw}^2R\right). \tag{4.2}$$

The value of the absorbed power is given as the time average of the product of $(h/2e)\,d\phi_{mw}/dt$ and the induced current $I_{mw}\cos(\omega_{mw}t)$. The parameter η which appears in Eq. (4.2) contains within it the weak-link characteristics I_c and ϕ_0—the equilibrium phase shift in the absence of microwaves, $\sin\phi_0 = I_0/I_c$:

$$\eta = \frac{I_c^2\cos^2\phi_0}{\left(\frac{1}{R}\frac{\hbar}{2e}\omega_{mw}\right)^2}. \tag{4.3}$$

We see from expressions (4.2) and (4.3) that P_n is the frequency-independent absorption in the normal state and that all of the frequency dependence is contained in the parameter η; this is in accordance with the experimentally observed frequency dependence of the low-field signal, mentioned earlier. It follows from the theory of the Josephson

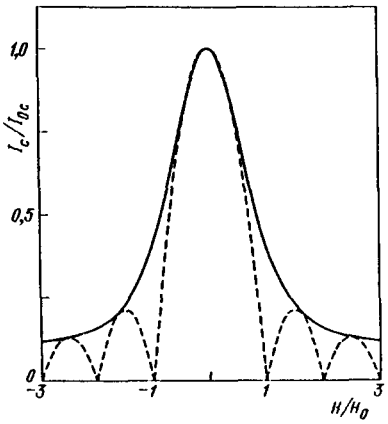

FIG. 13. Field dependence of the normalized critical current I_c/I_{c0} for an isolated Josephson contact (dashed curve) and for a network of weak links (solid current), according to expression (4.4). I_{c0} is the critical current in zero field.

effect that the field dependence of the critical current I_c of the contact obeys the diffraction relation (Fig. 13):

$$I_c(H) = I_{c0}\frac{\sin(\pi H/H_0)}{\pi H/H_0}, \tag{4.4}$$

where H_0 is the minimum value of the magnetic field, at which a Josephson contact of area S has a single magnetic flux quantum $H_0 S = 2.07\cdot 10^{-7}$ Oe·cm^2 passing through it. It is clear that the value of H_0 will be different for each individual Josephson unit; for the granular superconductor as a whole one can introduce a distribution function $F(H)$ describing the spread of the parameters of the weak links. The parameter η is then modified to $\eta(H) = \eta_0 F^2(H)$, where η_0 is the value of η in zero field, as is shown in Fig. 13.

The temperature dependence of the low-field signal intensity in this model is determined by that of the critical current $I_c(T)$ and, as we have said, depends strongly on the quality of the sample. Thus, for $T \leqslant T_c$ a Josephson medium exhibits a frequency-dependent absorption of microwave power, which is minimum in zero magnetic field and increases with the static magnetic field; this gives rise to a phase-inverted signal in zero field. It should be noted, however, that in fields exceeding the first critical field for the bulk superconductor, H_{c1}, vortices arise inside the superconducting granules as well. Therefore, for fields $H \geqslant H_{c1}$ ($H \geqslant 10^3$ Oe) an additional mechanism of absorption of the microwave field can arise, involving the pinning and depinning of vortices in the subsurface layer of the individual granules.[119]

It is a more complicated matter to take into account the effect of the low-frequency modulation H_M on the low-field signal. An additional term $I_M \cos(\omega_M t)$ arises on the right-hand side of Eq. (4.1). In Ref. 115 it was proposed to consider an exponential switching of the screening current from I_0 to $-I_0$ with a growth rate H^* as the external field H_{sc} is cycled. Under these conditions, because of the sign-varying behavior of ϕ_0 (ϕ_0 changes sign over the modulation period if $H_M > H^*$), the parameter η and the absorbed microwave power must behave nonlinearly. However, if the amplitude of the modulation is substantially smaller than H^*, one can treat the response of the system in a linear approximation.

To describe such a situation it has been proposed to use the simple expansion $F(H + H_M(\omega_M t)) \approx F(H) + F'(H) H_M \cos(\omega_M t)$. When this expansion is substituted into Eq. (4.1), one obtains in the adiabatic approximation at low modulation frequencies the following expression for the low-field signal amplitude $A_{1M} = P_{1M}{}^{1/2}$, where P_{1M} is the microwave power detected at frequency ω_M:[114]

$$A_{1M} = \frac{P_n^{1/2}}{\left(\frac{1}{R}\frac{\hbar}{2e}\omega_{mw}\right)^2}\frac{I_c}{(1+\eta)^{3/2}}\left(-\frac{dI_c}{dH}H_M + I_M \sin\phi_0\right). \tag{4.5}$$

We note that the field dependence and temperature dependence of the low-field signal are determined, as before, by the behavior of $I_c(H,T)$, and for synchronous detection the first term gives the derivative of the square of the critical current

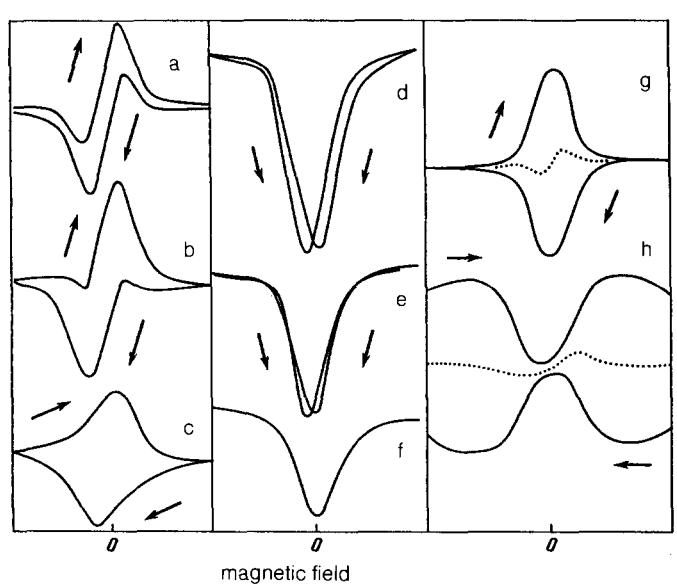

FIG. 14. Shape of the low-field signal at the first and second harmonics (A_{1M} and A_{2M}) for different values of the modulation amplitude and the parameter η (Ref. 114). The low-field signal at the first harmonic (ω_M) was 1 Oe (a), 0.32 Oe (b), and 0.10 Oe (c), and that at the second harmonic ($2\omega_M$) was 1 Oe (d), 0.32 Oe (e), and 0.1 Oe (f). Signals (g) and (h) were calculated from Eq. (4.5), with the parameter $\eta = 0.7$ and 70, respectively. The dotted curve gives the contribution from the term symmetric in the magnetic field in Eq. (4.5).

$-\mathrm{d}(I_c)^2/\mathrm{d}H$, while the second term, which is due to the modulation, changes sign upon the switching of the scanning field H_{sc} ($\phi_0 \to -\phi_0$), giving rise to hysteresis of the low-field absorption. As the temperature is lowered and, accordingly, η_0 increases, there is an increase in the amplitude and a broadening of the signal due to the first term of (4.5) and a simultaneous decrease in the contribution from the second term; the field dependence of the irreversible contribution has a minimum at zero field. The results are shown in Fig. 14g,h. The superposition of the two contributions, which is shown in Fig. 14a-c, is in good agreement with the experimentally observed behavior of the low-field signal in yttrium ceramics.[111,114,115,129]

Moreover, for a fixed modulation amplitude (i.e., I_M) there always exists a value of the magnetic field above which the condition $I_M \ll I_0$ breaks down, and the response becomes substantially nonlinear owing to oscillations of the phase ϕ_0. For large modulation amplitudes, just as for high magnetic fields, the contribution of the second term will saturate as a result of the nonlinearity of the system. In an analogous way one can consider the evolution of the low-field signal as the microwave power is increased, i.e., for large values of the current I_{mw}. Such an analysis will be carried out in greater detail for the low-field signal in single crystals of $YBa_2Cu_3O_{7-\delta}$. Thus in a physical sense the irreversible term is the first harmonic of the nonlinear response of the granular superconductor to a low-frequency modulation of the magnetic field.

Let us discuss the most important aspects of the response of the system at the second harmonic. According to direct calculations in the model under study, the amplitude of the absorption signal at the second harmonic ($2\omega_M$) is of the form[114]

$$A_{2M} = A_0\left[I_M^2 - \left(\frac{\mathrm{d}I_c}{\mathrm{d}H}\right)^2 H_M^2 - \frac{\mathrm{d}^2 I_c}{\mathrm{d}H^2} I_c H_M^2 + \frac{3}{1+\eta}\frac{1}{\left(\frac{\hbar\omega_{mw}}{2eR}\right)^2}\left(I_0 I_M - \frac{\mathrm{d}I_c}{\mathrm{d}H}H_M\right)^2\right], \tag{4.6}$$

where the coefficient A_0 corresponds to the factor in front of the parentheses in Eq. (4.5). The first three terms in (4.6), which are reversible in the magnetic field, form the absorption signal. The fourth term is reversible at low modulation amplitudes ($\propto I_0$) but acquires a hysteretic character for $I_M \gg I_0$. A superposition of the contributions shown in Fig. 14,d–f gives a good description of the experimental results on the low-field signal at the second harmonic of the low-frequency modulation.[111,114,129]

4.3. Low-field signal in single crystals of high-temperature superconductors

The bulk of the published results on microwave absorption in single crystals of high-temperature superconductors pertains to yttrium systems $YBa_2Cu_3O_{7-\delta}$ (Refs. 108, 109, 116–118, 120–122). The experimental data obtained in these studies, like those on the low-field signal in ceramics, indicate that the low-field microwave absorption is related to anomalies of the real structure of the single-crystal samples and is not correlated with the bulk superconducting properties.

For example, in the same single crystal of $YBa_2Cu_3O_{7-\delta}$ three low-field signals of different form (*A*, *B*, and *C* in Fig. 15) and with a different temperature dependence have been observed[141] in different temperature intervals below T_c. Similar signals have been observed separately in single-crystal high-temperature superconductors in several studies.[111,130] A separate series of low-field signals, regular in the magnetic field, has been observed[120–122] in twinned single crystals of $YBa_2Cu_3O_{7-\delta}$ (we shall call these type-*D* signals). We note that the low-field signal which is characteristic of ceramic yttrium systems apparently cannot be obtained by a simple superposition of the signals mentioned above.

Signal *A*, which is shown in Fig. 15A, is observed in $YBa_2Cu_3O_{7-\delta}$ single crystals prepared by the technology described in Ref. 142. The orientation dependence of its width ΔH_{pp} exhibits a divergence when the external magnetic field is oriented in the (*ab*) plane of the crystal, in which case the signal is not observed ($\Delta H(80°) = 44$ Oe), and a weak dependence in the interval $-50° \leqslant \alpha \leqslant +50°$, $\Delta H(\alpha) \approx 10$ Oe, where α is the angle between the field and the *c* axis of the crystal. Moreover, the amplitude of this signal has an unusual temperature dependence: when the signal first arises at $T \leqslant T_c$ it increases rapidly, reaches a maximum at $T_{max} \approx 85$ K, and then decreases to 0 as the temperature is lowered to $T \approx 75$ K, where the signal vanishes (Fig. 16A). The range of variation of the amplitude in this temperature interval is two orders of magnitude. The characteristic features of the type-*A* signal are the presence of extended wings, which approach the zero line in fields $H \approx 2$ kOe, and the absence of hysteresis.

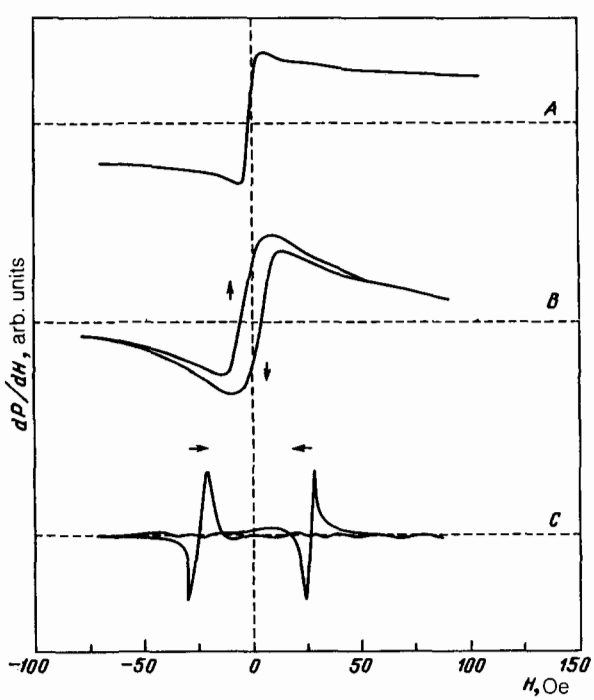

FIG. 15. Three types of low-field signals (*A*,*B*,*C*), observed in $YBa_2Cu_3O_{7-\delta}$ single crystals for $T \leqslant T_c$. The external magnetic field is oriented along the *c* axis of the crystal, and the magnetic component of the microwave field lies in the (*ab*) plane (Ref. 141).

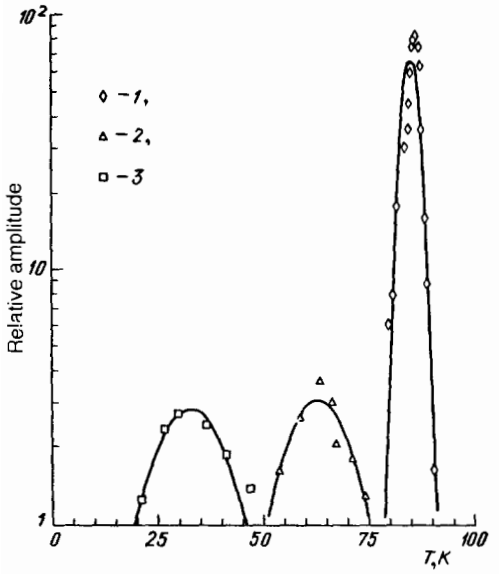

FIG. 16. Temperature dependences of the amplitude of signals of type A (1), B (2), and C (3), the shapes of which are shown in Fig. 15. The continuous curves joining the points are a quadratic interpolation of the experimental data.

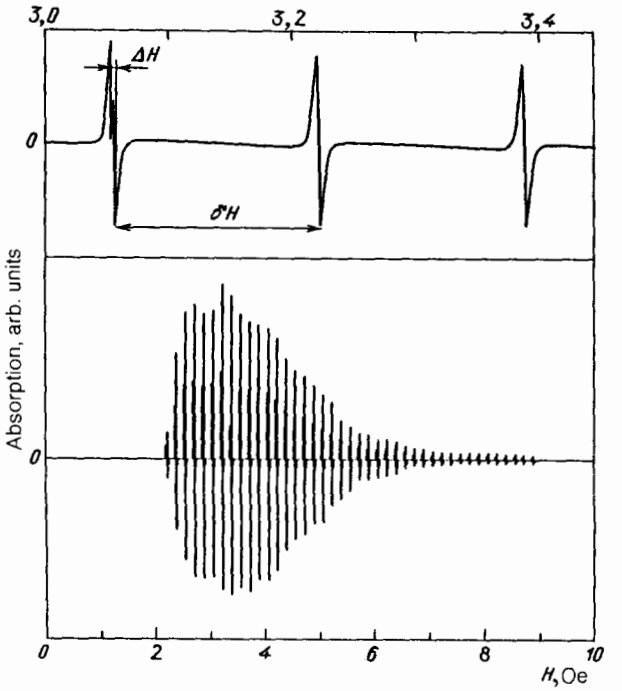

FIG. 17. Series of type-D signals observed in twinned single crystals of $YBa_2Cu_3O_{7-\delta}$. The external magnetic field is parallel to the [110] direction in the crystal. The magnetic component of the microwave field is parallel to the c axis. The power of the microwave field is 40 dB of 200 mW, $T = 4.4$ K (Ref. 120). The upper inset shows a three-line fragment of the series. The parameter δH characterizing the distance between lines equals 0.212 Oe. The characteristic width of an individual line is $\Delta H \approx 0.01$ Oe.

Signal B, which has a similar angular dependence, reaches maximum intensity at $T \approx 60$ K and is observed, as shown in Fig. 15B, in a lower temperature region, 50 K $< T <$ 75 K (see Fig. 16B). Its characteristic features are the absence of extended wings and the presence of hysteresis at zero field (G(64 K) = 10 Oe).

Signal C (see Fig. 15C), which is observed in the interval 20 K $< T <$ 50 K, reaches maximum intensity at $T_{max} = 30$ K; its width is several times smaller than the corresponding values for the low-field signals of types A and B. At high temperatures, $T > 40$ K, an unresolved structure appears, and the amplitude gradually falls to the noise level (see Fig. 16C). A characteristic feature of the type-C signal is the presence of appreciable hysteresis, which increases at low temperatures, $G(36\ \text{K})/\Delta H_{pp}\ (36\ \text{K}) = 10$.

The type-D signals differ both in the conditions of observation and in the behavior of their parameters. As we have said, they are obtained in specially prepared single crystals of $YBa_2Cu_3O_{7-\delta}$ which are threaded by a regular network of twins, and their phase corresponds to an EPR absorption signal.[117,118] In the case studied, the twins were oriented at an angle of 45° to the edge of the crystal (along the (110) direction in the crystal). The characteristic distance between twins was 1 μm.

The spectra in the field interval $0 \leqslant H \leqslant 10$ Oe at helium temperatures exhibited a regular series of isolated equidistant narrow lines, $\Delta H_{pp} \approx 2$ mOe, the distance between which was $\delta H = 245$ mOe. The typical form of the spectrum is shown in Fig. 17. The given structure arises when the external magnetic field is oriented along the (110) direction in the (ab) plane and vanishes for the perpendicular orientation in the same plane. The direction of the magnetic component of the microwave field here was parallel to the c axis of the crystal. When the magnetic component of the microwave field was oriented in the (ab) plane and the external field H was along the c axis, a sequence of narrow lines was likewise observed, but their field dependence was different from that described above.

In Ref. 122 a direct correlation between δH and the thickness of the $YBa_2Cu_3O_{7-\delta}$ single crystal was reported. For example, after the initial crystal 100 μm thick was separated into two thinner ($\approx 50\ \mu$m) layers as a result of thermal cycling, the distance between the D lines doubled from 245 mOe to 500 mOe. Moreover, the observation of fragments of the regular series of type-D low-field signals has been reported for a number of multidomain crystals of conventional type-II superconductors, $PbMo_6S_8$ and Nb, and reproducible series of intense lines of type D have been detected in fields above 50 Oe in thin ($\approx$50–100 μm) niobium crystals.[121] At the same time, these signals were not observed in hot-rolled samples.

The orientation dependences of an individual series of D lines in $YBa_2Cu_3O_{7-\delta}$ single crystals at different values of the external field is described by a universal relation:

$$H \cos\beta = \pm \left(p + \frac{1}{2}\right) H_0, \quad p = 1, 2, 3, \ldots, N, \qquad (4.7)$$

where β is the angle between the external field H and the (110) direction, and H_0, which was introduced in Eq. (4.4), is the minimum distance between lines. The corresponding data are shown in Fig. 18. In niobium crystals an analogous, though more complex, angular dependence at a fixed value of the external field arises about the preferred internal direction (α_0, β_0), associated with the predominant orientation

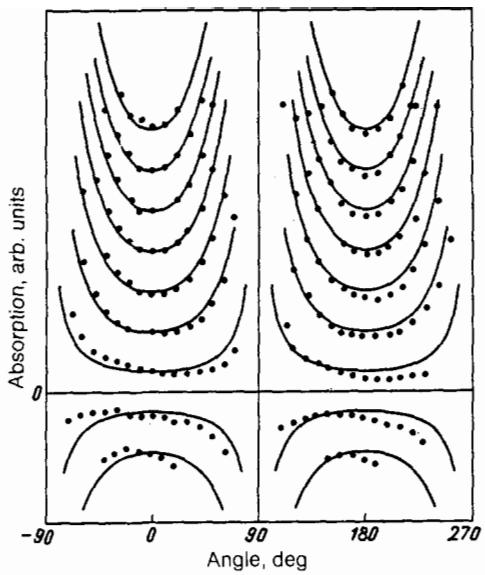

FIG. 18. The orientation dependence for an individual series of type-D lines in a $YBa_2Cu_3O_{7-\delta}$ single crystal 50 μm thick, $\delta H = 212$ mOe. The angle β is measured from the [110] direction in the (ab) plane of the crystal, so that 90° corresponds to an orientation of the external magnetic field along the [100] axis. The solid curves are the result of a numerical calculation according to Eq. (4.9) for several values $|p| = 1$–7 (Refs. 120–122).

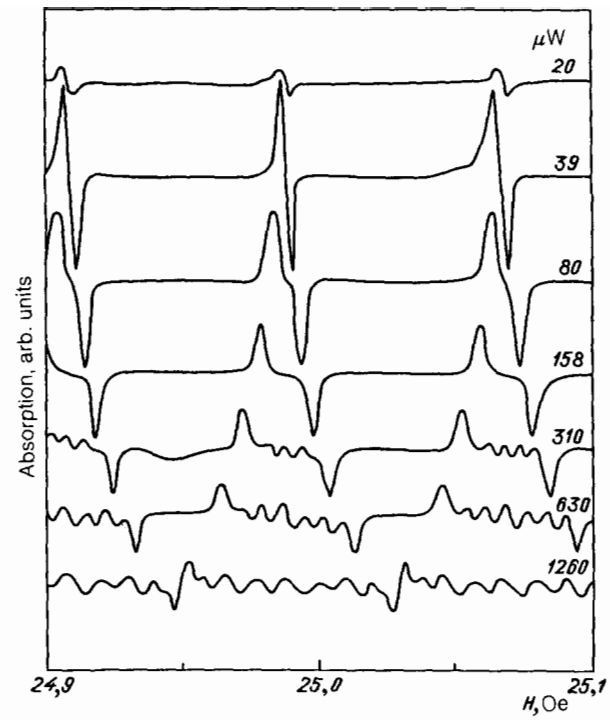

FIG. 19. Evolution of a fragment of a series of type-D lines as the power of the microwave field is increased from 20 μW to 1260 μW. At high powers ($P \geqslant 160\,\mu$W) the width ΔH is defined as the distance between the peaks on the positive and negative "halves" of the initial signal. We see that the phase-inverted signal in a field of 24.95 Oe at $P = 1260\,\mu$W is a result of the overlapping of two neighboring inhomogeneously broadened lines (Ref. 122).

of weak links in the sample (α_0 and β_0 are the direction angles in spherical coordinates).[120,121]

A substantial difference of the type-D signals from the low-field signal described earlier is the complex behavior of the parameters as functions of the microwave power P. Figure 19 shows the evolution of a fragment of the spectrum for various values $P = 20, 39, 80, 158, 310, 630$, and $1260\,\mu$W. It follows from the figure that as the microwave power is increased an inhomogeneous broadening of the initial signal occurs, with the formation of an expanding flat segment at the center of the line. At powers $P \geqslant 80\,\mu$W the linewidth can be characterized by the distance between the upper and lower halves of the derivative signal dP/dH. The slight structure in the absorption band for an individual line apparently forms the "mesosignal" that has been observed by a number of investigators in $MeBa_2Cu_3O_{6+\delta}$, where Me = Y, Ho, Eu.[106] The "inverted" signal arising between the centers of two neighboring lines at $P = 1260\,\mu$W is nothing other than the crossing of two inhomogeneously broadened lines. As the power is increased further a new series of type-D lines, characterized by a different value of the structure constant δH_2 than that of the previous series, appears; these lines in turn are broadened and overlap at high microwave powers. This behavior is shown in Fig. 20, and the corresponding dependence of ΔH is shown in Fig. 21. An analogous picture of the onset of a sequence of different series of D lines arises as the temperature is raised at a constant microwave power (see Fig. 22). By extrapolating the dependence of ΔH_{pp} on the microwave power to zero (see Fig. 21) one can determine for each line in the sequence the threshold power P_c below which that particular line is not observed. Plots constructed in this way, showing the dependence of P_c on the

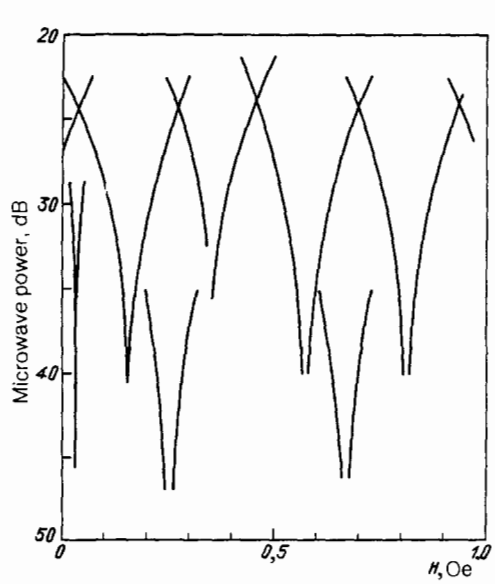

FIG. 20. Positions of the peaks on the positive and negative "halves" of a type-D signal as the microwave power increases. It is seen that as the attenuation coefficient is decreased below a threshold value of 40 dB a new series of lines appears, with a different value of δH than before. The lines of the new series broaden and overlap as the microwave power is increased further (the initial power was 200 mW; Ref. 120).

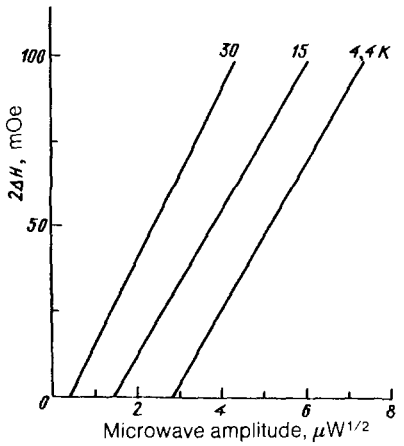

FIG. 21. Width ΔH of an individual line as a function of the amplitude of the microwave field for $T = 30$ K, 15 K, and 4.4 K (Ref. 121).

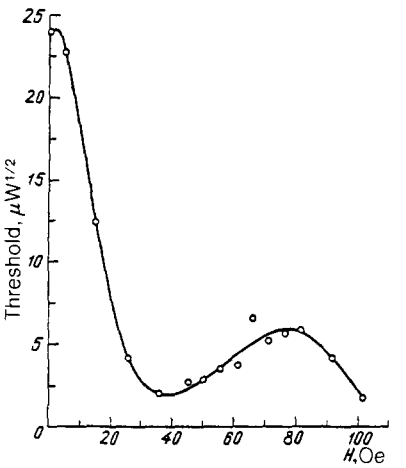

FIG. 23. Threshold amplitude of the microwave field for an individual series of type-D lines in $YBa_2Cu_3O_{7-\delta}$ single crystals ($T = 4.3$ K) as a function of the external magnetic field (Ref. 122).

magnetic field and temperature and characterizing the detailed evolution of the entire series of lines, are shown in Figs. 21 and 23. We note that for several values of the magnetic field the threshold microwave power for the onset of the series of lines is close to zero.

Thus the set of experimental data presented here has revealed the characteristic behavioral traits of the low-field signal in $YBa_2Cu_3O_{7-\delta}$ single crystals, viz., the appearance of low-field absorption signals of various types, depending on the technology of preparation of the single-crystal samples, their geometric factors, the configuration of the fields in the experiment, the temperature, and the microwave power. The observed properties are characteristic not only for $YBa_2Cu_3O_{7-\delta}$ but also for a number of conventional type-II superconductors with certain mechanical properties. Thus the mechanism of low-field absorption in single crystals of high-temperature superconductors, as in the case of ceramics, can be identified as the dissipation of microwave field energy in Josephson weak links formed by defects in the samples. Moreover, it is of interest to note that the observed characteristics can be linked to a specific form of defect, viz., twinning planes.

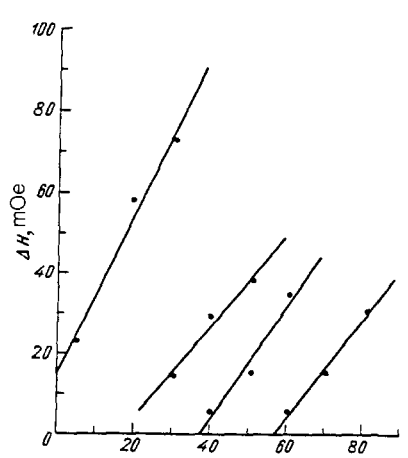

FIG. 22. Temperature dependence of ΔH for several series of lines in $YBa_2Cu_3O_{7-\delta}$ single crystals at an attenuation of 42 dB ($P = 200$ mW; Ref. 120).

4.4. Model of the formation of the low-field signal in $YBa_2Cu_3O_{7-\delta}$ single crystals

The existence of a common orientation dependence of the form (4.7) allows one to attribute the observed series of D lines to the penetration of the magnetic flux lines into the weak links. On the other hand, the strict periodicity in the magnetic field suggests the existence of crossing energy levels, corresponding to states with different numbers of vortex lines inside the bounded space of the weak-link unit. In other words, a fragment of a twinned single crystal can be regarded as an isolated quantum interferometer.

In the case investigated in Ref. 121 the boundaries of the weak link are planes lying perpendicular to the surface of the crystal and separated by a distance of 1 μm. The effects of disorientation in neighboring domains are apparently not important.

The magnetic energy of a cluster consisting of weakly linked superconducting granules, according to the theoretical model of Ref. 131, have a periodic quadratic dependence on the external magnetic field, with a period equal to H_0, the minimum field at which a single magnetic flux quantum passes through the surface of the cluster:

$$u_n = \frac{1}{8\pi}(H - nH_0)^2 fS, \tag{4.8}$$

where f is the Meissner factor, S is the area of the effective surface, and n is the number of flux quanta. We note that the weak links in single crystals are more regular and have substantially smaller geometric dimensions than in the case of ceramics. For the single crystals described, with $d = 100$ μm, the area of an isolated boundary is 10^{-6} cm^{-2} and the corresponding minimum field is $H_0 = 200$ mOe. Separating the initial crystal into two layers of thickness $d = 50$ μm doubles the field to $H_0 = 400$ mOe. These estimates are in good agreement with the measured values of δH for the given crystals. A graphical representation of expression (4.8) is shown in Fig. 24. If the viscous motion of vortex lines at the

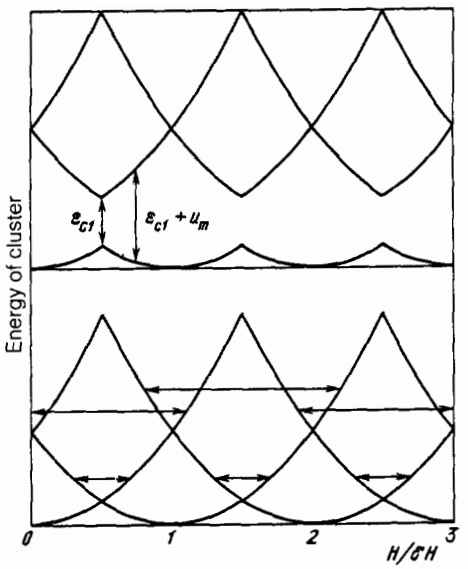

FIG. 24. Diagram of the energy of a superconducting cluster as a function of the external magnetic field, constructed according to Eq. (4.8) without allowance for the gap (lower diagram) and with allowance for the energy of formation of a Josephson vortex, ε_{c1} (upper diagram). The term u_m characterizes the magnetic energy of a vortex at intermediate values of the field. The horizontal lines on the lower diagram indicate the width of the individual lines in the series at several different values of the microwave power. The overlap of the lines reflects the overlap of the inhomogeneously broadened signals shown in Figs. 20 and 21 (Refs. 120–122).

site of the level crossing is taken as the possible mechanism for the dissipation of microwave power (for such a dissipation the magnetic energy is completely converted into kinetic energy of vortex motion, $(\frac{1}{2})\ mV^2$, where m is the effective mass of a vortex), then one would expect that with increasing power the absorption linewidth $\Delta H_{pp} \approx \Delta H(P)$ would increase in proportion to the distance between neighboring energy levels:[120]

$$\Delta H = \left(\frac{8\pi u_m}{fS}\right)^{1/2} - \frac{\delta H}{2}. \tag{4.9}$$

Thus the microwave field stabilizes the intermediate state of the weak link. Further increase in the microwave power will cause inhomogeneous broadening of the initial absorption line, $\Delta H \sim P^{1/2}$ and the subsequent overlapping of two or more neighboring lines, as is shown by the horizontal lines in Fig. 24.

The qualitative situation described is completely borne out in experiment (see Figs. 19–21), and the introduction of a threshold power parameter $P_c(T)$ allows one to describe the experimentally observed broadening in different series of lines by a simple dependence of the form

$$2\frac{\Delta H}{\delta H} = \left(\frac{P}{P_0}\right)^{1/2} - \left(\frac{P_c}{P_0}\right)^{1/2}, \tag{4.10}$$

where P_0 is a common parameter for the different series of lines and characterizes the temperature independent slope of the $\Delta H(P)$ curves.

The theory of the Josephson effect in a magnetic field[119,132] enables one to describe the critical current through a weak link that is necessary for the formation of a Josephson vortex in it:

$$J_0 = \frac{\pi}{4}\frac{2\Delta}{eR_n}\text{th}\frac{\Delta}{2k_BT}, \tag{4.11}$$

where $\Delta(T) \approx 1.74\Delta(0)\,[1-(T/T_c)]^{1/2}$ for $t \leqslant T_c$ is the energy gap in the BCS model, $2\Delta(0) = 3.528k_BT_c$, and R_n is the resistance of a unit surface of the Josephson contact. Taking the temperature dependence into account, we can simplify the form of expression (4.11):

$$J_0(T) \approx 2.67J_0(0)\left(1-\frac{T}{T_c}\right), \tag{4.12}$$

where the critical current $J_0(0)$ is determined solely by the parameters of the superconductor.

To produce a critical current (4.12) on the surface one must apply a microwave field with amplitude greater than or equal to the critical value h_{c1}:

$$h_{c1} \approx \frac{4\pi}{c}\lambda_J(T)J_0(T), \tag{4.13}$$

where λ_J is the penetration depth of the field into the Josephson contact:[132]

$$\lambda_J = \left(\frac{c\Phi_0}{8\pi^2J_0d}\right)^{1/2} \quad (d \ll 2\lambda_L) \approx \left[\frac{\Phi_0/4\pi}{(4\pi/c)\lambda_LJ_0}\right]^{1/2}, \tag{4.14}$$

where d is the size of the contact and λ_L (the expression for which is taken from Ref. 121) is the London penetration depth of the field into the volume of the superconductor. We will not examine the details of the temperature dependence of λ_J and h_{c1}, which derive from the temperature dependence of the fundamental parameters λ_L and Δ. It is clear that expressions (4.13) and (4.14) imply the existence of a threshold microwave power, viz., that which generates the critical current on the surface of the weak link. Moreover, the threshold power should have a monotonic temperature dependence, determined by the fundamental parameters; this is in complete agreement with the experimental data presented earlier.

The requirement that the critical current $J_0(T)$ for the formation of a Josephson vortex exist on the surface of the crystal may be reflected in the appearance of a gap ε_{c1} on the diagram for the magnetic energy of a cluster (see Fig. 24). It has been proposed,[121] by analogy with the energy density of fluxoid formation in a bulk superconductor, to write the corresponding energy associated with the critical current J_0 as $\varepsilon_{c1} = (1/4\pi)\Phi_0h_{c1} \simeq (I/c)\Phi_0\lambda_J(T)J_0(T)$. Then the total energy of a vortex will contain two components—the energy of formation ε_{c1} and the magnetic energy u_m, given by relations (4.8) and (4.9):

$$\varepsilon_1 = \varepsilon_{c1} + u_m. \tag{4.15}$$

If the magnetic energy u_m is defined as the difference $(u_{n+1} - u_n)$, where u is the magnetic energy of a cluster containing n and $(n+1)$ vortices, respectively, then u_m can be written in the form

$$u_m = u_{n+1} - u_n = 8u_0\left[(n+\tfrac{1}{2}) - \frac{H}{\delta H}\right] = 4u_0\frac{\Delta H'}{\delta H}, \tag{4.16}$$

where $u_0 = (I/32\pi)\Phi_0\delta H$ is the energy for the lowest crossing of levels $u(H)$. As we see from expression (4.16), the magnetic energy u_m depends only on the deviation of the magnetic field from its value at the point of the level crossing, $\Delta H'$. At the points $H = (n + 1/2)\delta H$ the energy of states with n and $(n + 1)$ fluxoids are equal, so that the magnetic energy associated with the creation of a vortex is zero at the threshold point. By making a term-by-term comparison of expressions (4.10), (4.13), (4.15), and (4.16) we can relate the parameters of the experiment with the parameters of the model:

$$h_1/\delta H = \left(P/P_0\right)^{1/2},$$
$$h_{c1}/\delta H = \varepsilon_{c1}/8u_0 = \left(P_c/P_0\right)^{1/2}. \tag{4.17}$$

Since, as we have said, δH is determined by the geometry of the weak links in the sample, the slope of the curves is indeed determined by the sample and is independent of temperature. At the same time, the threshold power is determined by the relationship between the energy of formation of a Josephson vortex and the functional form of the magnetic energy of a superconducting cluster (4.8). We note also that the value of $\Delta H'$ at which the relation $\varepsilon_1 = (I/4\pi)\Phi_0 h_1$ is satisfied is equal, within a constant factor, to the parameter ΔH_{pp} for an inhomogeneously broadened isolated line. The appearance of additional structure at the center of an individual line for $P \gg P_c$ (see Fig. 19) can then be attributed to the generation of two vortices by the microwave field.[122] For two-vortex generation one can in turn determine the threshold power P_{c2} and the value of $d\Delta H_{pp}/dP$ and construct a qualitative model similar to the previous one. However, the experimental data indicate that there are important differences between one-vortex and two-vortex generation. For example, for a one-vortex process in $YBa_2Cu_3O_{7-\delta}$ the value of $d\Delta H_{pp}/dP$ depends only weakly on the field within a given series and is about 2.6 mOe/$\mu W^{1/2}$, while for the secondary process it varies from 0.6 mOe/$\mu W^{1/2}$ in a field of 5 Oe to 0.25 mOe/$\mu W^{1/2}$ in fields above 50 Oe.[122] The features associated with two-vortex generation are not observed in niobium crystals.[121]

The connection between the energy of a Josephson vortex formed in a given magnetic field and the current induced by the microwave field can also account for the nonmonotonic field dependence of the threshold power $P_c(H)$. When a field is applied in an isolated contact with transverse dimension d, a lattice of Josephson vortices with a period $\lambda_B = \Phi_0/B(d + 2\lambda_L)$ is established. Starting from the fact that the total magnetic flux in the contact is equal to the trapped flux, for an individual contact of length L we obtain the relation $BL(2\lambda_L + d) = HS$. Assuming that the new vortex is created within the penetration depth λ_J of the microwave field into the weak link, we can write for J_c the expression[121]

$$J_c = \frac{J_0}{\lambda_J}\left|\int_0^{\lambda_J} \cos\frac{2\pi x}{\lambda_B}\,dx\right| = \frac{J_0\lambda_B}{2\pi\lambda_J}\left|\sin\frac{2\pi\lambda_J}{\lambda_B}\right|, \tag{4.18}$$

from which it follows that, under the condition $2\lambda_J = \lambda_B$, the critical current for the creation of a new vortex is zero.

Thus in fields $H_{J0} = n(L/2\lambda_J)\delta H$ the critical current for the formation of a new vortex, and, hence, the threshold microwave power, will be zero. This situation is in fact observed in experiment (see Fig. 23).

The assumption that the a vortex undergoes viscous motion under the influence of the magnetic component of the microwave field allows us to write its velocity as $V \sim h_1/\eta\lambda_{J\perp}$, where h_1 is the magnetic component of the microwave field, η is the viscosity of the vortex, and $\lambda_{J\perp}$ is the penetration depth of the field. At present there are several approaches used to estimate the viscosity of a vortex in a Josephson medium.[133,134,139] The use of the simplest expression,[135] $\eta \propto H_{c2}/\rho_{ab}$, where ρ_{ab} can be described by a relation linear in the temperature,[136] yields

$$2\Delta H = (\alpha + \beta T)h_1 - \delta H = \frac{\beta(T - T_0)}{\alpha + \beta T_0}\delta H, \tag{4.19}$$

where $\alpha^2 \sim (Q/SH_{c2})\,[\rho_{ab}(0)/\omega\lambda_{J\perp}] \simeq (0.15/f)Q$. The parameter $Q = \omega m/2\eta$ has the meaning of a quality factor. The most important properties of (4.19) are the linear temperature dependence, which derives from the linear dependence of the electrical conductivity in the (ab) plane, and the presence of a threshold temperature $T_0 = (\delta H/h_1 - \alpha)/\beta$, below which a given series of lines should not be observed.

A comparison of the experimental temperature dependence of ΔH and the results of an extrapolation of $\rho_{ab}(T)$ to zero temperature gives satisfactory agreement. Expression (4.19) also accounts for the appearance of series of lines in various temperature intervals at a fixed microwave power (see Fig. 22).

At the same time, there exist data which cast doubt on the assumption that the microwave power is dissipated through the viscous motion of a Josephson vortex. A study[121] of the behavior of P_c for different angles between the directions of the magnetic component of the microwave field h_1, the external field H, and the crystallographic axes of the sample in $YBa_2Cu_3O_{7-\delta}$ and niobium crystals indicates that the threshold microwave power is significantly larger in the case of a parallel orientation $h_1 \| H$. For niobium this angular dependence obeys the relation $P_c \sim 1/\sin^2(\alpha - \alpha_0)$, and P_c reaches a maximum at the same angle α_0 for which δH is minimum. This fact can be regarded as an indication that the formation of the series of type-D lines is due to the component of the induced microwave current parallel to the direction of the vortex.

4.5. Characteristics of the weak links

Expressions (4.13) and (4.14), which were used in the model for the formation of the type-D low-field signal, permit estimation of several characteristics of the Josephson contacts. From measurements of the threshold microwave power one can estimate h_{c1} and, hence (see Eq. (4.14)), the penetration depth λ_J. In Ref. 121 the corresponding estimates were made using values of the London penetration depth $\lambda_L(0) = 900$ Å determined from experiments on muon rotation in $YBa_2Cu_3O_{7-\delta}$ single crystals.[137,138] Expression (4.13) can then be used to estimate the critical current J_0.

Assuming the validity of the BCS model, we can estimate the resistance R_n of the tunnel contact:

$$R_n = R_0\exp(kd), \tag{4.20}$$

TABLE I. Characteristics of Josephson contacts in $YBa_2Cu_3O_{7-\delta}$ single crystals (Ref. 121).

T, K	h_{c1}, mOe	$\lambda_L(T)$, Å	J_0 A/cm^2	λ_J, μm	R_n, m$\Omega\cdot$cm^2
4,4	66	900	1,96	270	10,8
15	50	900	1,13	350	18,8
30	24	900	0,26	740	82,0
4,4	64	900	1,84	280	11,5
15	32	900	0,46	550	46,0
30	10	900	0,04	1800	470,0

where d is the transverse dimension of the contact and k is determined from the expression $hk = (2m\varepsilon_b)^{1/2}$; for an energy barrier $\varepsilon_b \approx 1$ eV one has $1/k \approx 2$ Å. Numerical values of the parameters h_{c1}, λ_J, J_0, and R_n corresponding to several series of lines at various temperatures are given in Table I.

5. HYSTERESIS OF THE MICROWAVE ABSORPTION

Hysteresis of the microwave absorption at $T < T_c$ was observed in the very first experiments on EPR in high-temperature superconductors.[32,143,144] This effect consists in the fact that the absorbed power depends on the scanning direction of the static magnetic field. Figure 25 shows a typical experimental hysteresis curve in $YBa_2Cu_3O_{7-\delta}$. As we know, when a type-II superconductor is placed in a magnetic field of intermediate strength $H_{c1} < H < H_{c2}$ (where H_{c1} and H_{c2} are the first and second critical fields) it undergoes a transition to a mixed state, i.e., the magnetic field enters a type-II superconductor in the form of quantum vortex filaments (Abrikosov vortices) that extend along the magnetic field lines. The hysteresis in the field dependence of the thermodynamic potentials for hard superconductors in the mixed state is due to pinning of these vortices on irregularities with sizes of the order of the radius of a vortex. Therefore, it is natural to suppose that the observed anomalies of the microwave properties are also due to pinning. However, the microwave hysteresis detected in EPR studies cannot be identified with the known hysteresis of the magnetization of superconductors, if only because the widths of the individual hysteresis loops differ by three orders of magnitude and the size of the effect in the case of EPR is incomparably smaller. Subsequent studies have shown that hysteresis of the microwave absorption is observed in a wide class of superconducting materials: $La_{1.8}Sr_{0.2}CuO_4$, V_3Si, Nb, and $NbSe_2$ (Ref. 32).

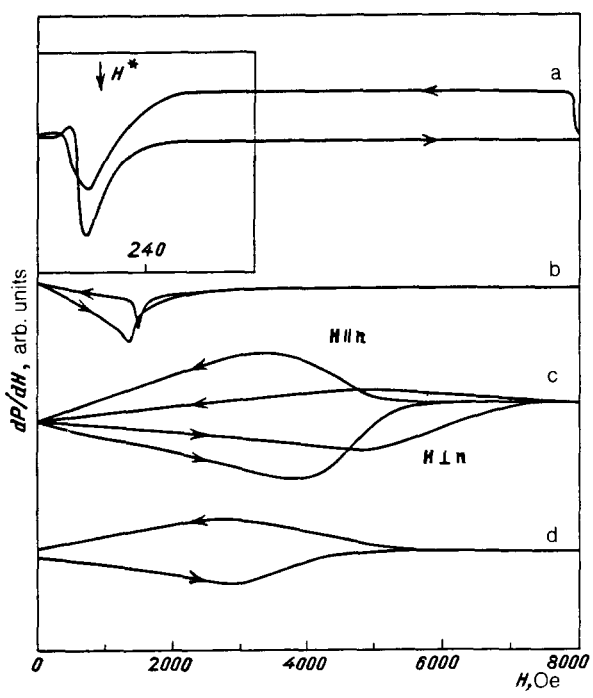

FIG. 25. Field dependence of the microwave absorption dP/dH for various samples in the superconducting state. a) $YBa_2Cu_3O_7$; b) perfect single crystal of Nb; c) hot-rolled Nb foil; d) deformed single crystal of Nb. The data were taken from Ref. 32.

Figure 25 shows the form of the microwave hysteresis for the following samples: b) a chemically polished perfect single crystal of niobium, with $R(4.2\text{ K})/R(300\text{ K}) = 300$; c) a slab of hot-rolled commercial-grade niobium; and d) a sample cut out from the same single crystal but without the chemical polishing. An important conclusion we can draw from the figure is that the possibility of observing the hysteresis effect depends on the degree of deformation of the superconductor, since the microwave hysteresis is absent in the polished Nb single crystal and is most pronounced in the foil. It has been shown[145] that the interaction of vortices with a microwave field is not complicated by pinning effects, and therefore the microwave absorption by a superconductor in a magnetic field will be determined by the number and distribution of vortices in the magnetic skin layer. In the Bean model of the critical state in a hard superconductor, upon any change in the magnetic field a critical state is established in which the current density (everywhere that it is nonzero) can be assumed equal to $j_c(T)$. The value of the critical current is determined from the condition for the onset of motion of the vortex structure. The statistical distribution of vortices in the sample (and at the skin depth, in particular) is established as a result of a balance of the pinning and Lorentz forces. A change in the scanning direction of the magnetic field causes a corresponding change in the direction of the critical currents, which because of the Lorentz force can squeeze the vortex into or out of the skin layer.

A number of parameters has been introduced for describing the hysteresis of the microwave absorption (Fig. 26): δ—the amplitude of the hysteresis (the difference between the microwave absorption levels for the different scanning directions of the magnetic field), ΔH—the width of the transition from the lower to the upper level of the particular hysteresis loop, and H^*—the upper magnetic field at which the microwave hysteresis vanishes.

The temperature dependence $\delta(T)$ measured for different superconductors has a "universal" character:

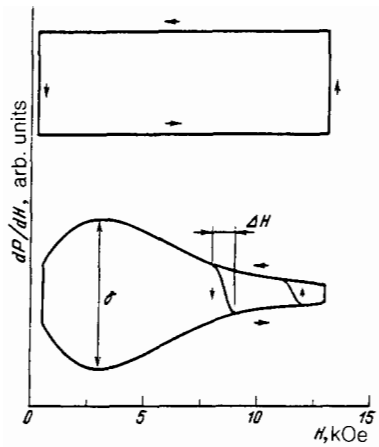

FIG. 26. Field dependence of the first derivative of the absorbed power dP/dH in a $YBa_2Cu_3O_{6.9}$ single crystal for two different orientations of its (ab) crystallographic plane relative to the direction of the static magnetic field H_0. Upper: $(ab)\perp H_0$; lower $(ab)\parallel H_0$. The arrows indicate the scanning direction of the magnetic field. $T = 5.0$ K.

$\delta(T) \sim [1-(T/T_c)^2]$ (Ref. 32). Such a temperature dependence is characteristic for the pinning force in dirty superconductors.[147] However, in the case of Y–Ba–Cu–O the temperature dependence $\delta(T)$ differs from the universal form (Fig. 27). The cause of this difference has become clear after a study[33] was made of a series of $YBa_2Cu_3O_{7-x}$ samples with different oxygen contents $x = 0.04$, 0.14, 0.31, 0.44, and 0.56. The data on $\delta(T)$ for these samples are shown in Fig. 27. It follows from this figure that the subsurface region of samples of stoichiometric composition contains a phase with a lower T_c (~ 60 K), which gives rise to screening effects that cause $\delta(T)$ to be nonmonotonic. We note that in the region $T_c \sim 60$ K there is a plateau on the $T_c(x)$ curve (see Fig. 2).

The behavior of the microwave hysteresis parameter ΔH depends importantly on the type and state of the superconductor. While in the case of Y–Ba–Cu–O ceramic samples this quantity is very small and does not exceed 0.01 Oe,

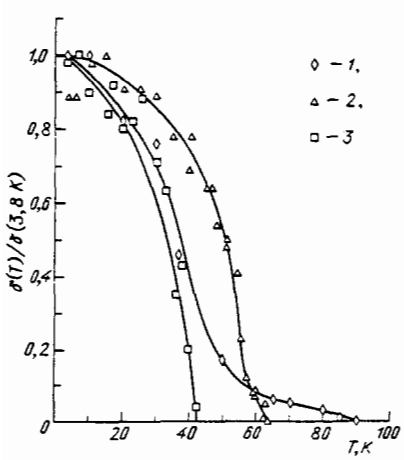

FIG. 27. Temperature dependence of the normalized amplitude of the hysteresis $\delta(T)/\delta(3.8\ \text{K})$ for $YBa_2Cu_3O_x$ compounds with different oxygen contents: *1)* $x = 6.96$; *2)* $x = 6.86$; *3)* $x = 6.60$.

for niobium single crystals it is approximately 40 Oe. In terms of the Bean approach one can conjecture[32] that $\Delta H = \zeta j_c$, where ζ is the coherence length. For niobium this formula gives a value of j_c that is in satisfactory agreement with the results of other experiments.

In Y–Ba–Cu–O single crystals the temperature and field dependences of the microwave hysteresis parameters depend on the orientation of the crystal relative to the magnetic field direction.[34] The complicated orientation dependence of the hysteresis amplitude δ in a single crystal apparently stems from a superposition of two antagonistic contributions. One of these is the anisotropy of the penetration depth of the magnetic field, which is 5 times larger along the c axis than in the (ab) plane;[12] the other is the predominant pinning of the vortices in the (ab) plane as a result of the strong twinning of single crystals in this plane. Using the formula for ΔH given above with the data on the penetration depth in the single crystal,[12] we can estimate the critical current as $j_{c(ab)}(20\ \text{K}) = 3\cdot 10^6\ \text{A/cm}^2$, $j_{c(c)}(20\ \text{K}) = 8\cdot 10^4\ \text{A/cm}^2$; these values are in good agreement with the values determined from the data on the width of the hysteresis loop of the magnetization. The data on the upper field at which the hysteresis vanishes, H^*, for the single crystal are in satisfactory agreement with the values of the second critical field measured by other methods.

6. CONCLUSION

A little more than 5 years have passed since the discovery of high-temperature superconductivity, and in spite of the progress made in the search for new superconductors with higher values of T_c, the main questions confronting our understanding of the physics of this phenomenon still have not been answered unambiguously. The main difficulty here is the contradictory nature of the experimental results. The data obtained in EPR studies are also contradictory and ambiguous. Nevertheless, we shall attempt to state several conclusions.

1. No EPR signal is observed from superconducting YBaCuO compounds. The absence of a signal is apparently due to the strong exchange interaction both between the magnetic moments of Cu^{2+} and between them and the spins of the current carriers.

2. For oxygen-deficient nonsuperconducting YBaCuO compounds the inconsistency of the experimental results is most likely due to the fact that for intermediate (between 6 and 7) oxygen concentrations there exist several possible metastable microscopic configurations in the oxygen distribution, depending largely upon the annealing temperature of the sample. The observed EPR signal is due to localized magnetic moments of Cu^{2+} in the Cu1 positions (chains). No signal is observed from the Cu2 localized moments, which arise on neutron bombardment, for example, because of the strong antiferromagnetic exchange interaction between them.

3. The introduction of rare-earth magnetic impurities (Gd^{3+}, Eu^{3+}, Hf^{3+}, Ho^{3+}, etc.) in YBaCuO does not give the expected results as to the determination of the superconducting parameters of the system, since the ytterbium and the ions replacing it interact weakly with the conduction electrons and have only a slight effect on the superconducting properties.

4. The change in the temperature dependence of the EPR linewidth for localized moments of DPPH adsorbed on the surface of a high-temperature superconductor has permitted calculation of the temperature dependence of the penetration depth of the magnetic field into the superconductor.

5. The nonresonant absorption of microwave power by ceramic and single-crystal samples in low magnetic fields is attributed by most authors to the presence of a network of Josephson weak links in the sample. The substantial difference in the nature of the low-field signal from ceramics and single crystals is a consequence of the different nature of the dominant weak links, which are intergranular links in the case of ceramics and twinning planes or microcracks in the case of single crystals.

6. The origin of the low-field signal in ceramics is ordinarily attributed to dissipation of microwave power as the external magnetic field increases, due to modulation of the phase of the screening microwave surface current. In contrast, the periodic sequence of narrow absorption signals in single crystals corresponds to the penetration of Josephson vortices into a regular lattice of weak links. In this case the single crystal acts as a quantum interferometer. In intermediate cases (compacted ceramic, poor-quality single crystals) both mechanisms are apparently operative.

7. The magnetic hysteresis of the microwave absorption observed in EPR experiments is due to pinning of Abrikosov vortices. Measurements of the parameters of this hysteresis have permitted estimation of the critical currents and the quality of the sample surface.

One of the remaining tasks for EPR studies is to investigate YBaCuO samples with different oxygen content, since it is quite probable that EPR will be a convenient tool for differentiating between samples having the same oxygen content but different types of oxygen ordering. This would afford the possibility of investigating metastable states of YBaCuO, including superconducting states.

An attractive direction for further research is the development of techniques for studying the vortex state of superconductors with the aid of EPR decoration of the surface. However, the accuracy of the data obtained will be degraded considerably by the complexity of taking pinning effects into account in the calculation of λ.

As we have tried to show, there has been certain progress made toward understanding the nature of the low-field signal in high-temperature superconductors. At the same time, the interpretation given in this article to the nonresonant microwave absorption in low magnetic fields does not exhaust all the existing points of view. For example, a number of authors[43] have examined the possibility that the observed low-field anomaly in the absorption is due to the onset of the first critical field H_{c1}. Others have convincingly demonstrated the existence of a low-field signal in type-I superconductors below T_c. In this case the most probable mechanism responsible for the absorption is the field dependence of the penetration depth of the microwave field into the superconductor.[124,125] This explanation of the effect does not require the presence of a vortex lattice.

Of particular importance are recent experiments in which an intense low-field signal has been observed in systems that do not have a superconducting state ($Gd_{2-x}Sr_xCuO_4$, $EuTbCuO_4$, etc.).[109,110] It was noted by the authors of those studies that the low-field signal in these compounds also has an inverted phase and exhibits hysteresis in zero field. The only distinguishing feature of the new signal from the low-field signal in superconductors is the inverted sign of the hysteresis. At present there is no consistent interpretation of the effect, and most authors are inclined to attribute this signal to a peculiarity of the magnetic state of the systems.

We have not attempted to cover all the approaches in this one article but have tried to clarify the more or less established experimental facts and models. Moreover, we have focused on the results that have been most completely published and widely discussed.

Finally, we note that the study of the nature of the low-field signal substantially enriches the possibilities of the conventional EPR technique, and in the search for new superconductors the detection of the low-field signal affords a highly sensitive test of trial samples for the presence of small inclusions of a superconducting phase inside them.

In closing, we thank I. A. Garifullin, A. Dulcic, F. Meran, and A. M. Portis for providing materials and for discussion.

[1] J. G. Bednorz and K. A. Müller, Rev. Mod. Phys. **60**, 585 (1988).
[2] A. I. Golovashkin, Usp. Fiz. Nauk **152**, 553 (1987) [Sov. Phys. Usp. **30**, 659 (1987)].
[3] L. P. Gor'kov and N. B. Kopnin, Usp. Fiz. Nauk **156**, 117 (1988) [Sov. Phys. Usp. **31**, 850 (1988)].
[4] B. K. Chakraverty, M. Avignon, and D. Feinberg, J. Less-Common Met. **150**, 11 (1989).
[5] Yu. A. Izyumov, N. M. Plakida, and Yu. N. Skryabin, Usp. Fiz. Nauk **159**, 621 (1989) [Sov. Phys. Usp. **32**, 1060 (1989)].
[6] M. Yu. Kupriyanov and K. K. Likharev, Usp. Fiz. Nauk **160**(5), 49 (1990) [Sov. Phys. Usp. **33**, 340 (1990)].
[7] B. M. Khabibullin and E. G. Kharakhash'yan, Usp. Fiz. Nauk **111**, 483 (1973) [Sov. Phys. Usp. **16**, 806 (1974)].
[8] K. Baberschke, Z. Phys. B **24**, 53 (1976).
[9] S. E. Barnes, Adv. Phys. **30**, 801 (1981).
[10] R. L. Cava, A. W. Hewatt, E. A. Hewatt, B. Batlogg, M. Marezio, K. M. Rube, J. J. Krajewski, W. F. Peck, and L. W. Rupp Jr., Physica C **165**, 419 (1990).
[11] B. A. Aleksashin, A. M. Bogdanovich, S. V. Verkhovskiĭ, Yu. I. Zhdanov, V. L. Kozhevnikov, K. N. Mikhalev, K. A. Okulova, A. A. Romanyukha, A. M. Serikov, A. M. Sorkin, V. A. Tsurin, S. M. Cheshnitskiĭ, Yu. N. Shvachko, V. I. Anisimov, M. I. Katsnel'son, A. L. Likhteĭnshteĭn, A. V. Trefilov, and S. A. Turzhevskiĭ, Pis'ma Zh. Eksp. Teor. Fiz. **48**, 263 (1988) [JETP Lett. **48**, 289 (1988)].
[12] Y. Iye, Tech. Rep. ISSP Ser. A., No. 2058 (1988).
[13] K. R. Krylov, A. I. Ponomarev, I. M. Tsidilkovskiĭ, V. I. Tsidilkovskiĭ, G. V. Bazuev, V. L. Kozhevnikov, and S. M. Cheshnitskiĭ, Phys. Lett. A **131**, 203 (1988).
[14] R. J. Cava, B. Batlogg, R. B. van Dover, D. W. Murphy, S. Sunshine, T. Siegrist, J. P. Remeika, E. A. Rietman, S. Zahurak, and G. R. Espinosa, Phys. Rev. Lett. **58**, 1676 (1987).
[15] Y. Bruynseraede, J. Vanacken, B. Wuyts, C. van Haesendonck, J.-P. Locquet, and I. K. Schuller, Phys. Scr. **29**, 100 (1989).
[16] Y. Ueda and K. Kosuge, Physica C **156**, 281 (1988).
[17] P. Monod, M. Ribault, F. D'Yvore, J. Jegouder, G. Collin, and A. Revcolevschi, J. Phys. (Paris) **48**, 1369 (1987).
[18] P. P. Freitas and T. S. Plaskett, Phys. Rev. B **36**, 5723 (1987).
[19] J. M. Tranquada, A. H. Moudden, A. I. Goldman, P. Zolliker, D. E. Cox, G. Shirane, S. K. Sinha, D. Vaknin, D. G. Johnston, M. S. Alvazer, A. J. Jacobson, J. T. Lewandowski, and J. M. Newsam, Phys. Rev. B **38**, 2477 (1988).
[20] I. V. Aleksandrov, A. P. Volodin, I. N. Makarenko, L. E. Svistov, and S. M. Stishov, Pis'ma Zh. Eksp. Teor. Fiz. **49**, 287 (1989) [JETP Lett. **49**, 327 (1989)].
[21] Y. Nakazawa and M. Ishikawa, Physica C **158**, 381 (1989).
[22] G. Cannelli, R. Cantelli, F. Cordero, and M. Ferritti, Solid State Commun. **68**, 323 (1988).
[23] Y. Takeda, R. Kanno, O. Yamamoto, M. Takano, Z. Hiroi, Y. Bando, M. Shimada, H. Akinaga, and A. Takita, Physica C **157**, 358 (1989).
[24] K. N. Tu, N. C. Yeh, S. I. Park, and C. C. Tsuei, Phys. Rev. B **39**, 304 (1989).

[25] W. K. Kwok, G. W. Crabtree, A. Umezawa, B. W. Veal, J. D. Jorgensen, S. K. Malik, L. J. Nowicki, A. P. Paulikas, and L. Nunez, Phys. Rev. B **37**, 106 (1988).
[26] A. T. Fiory, Phys. Rev. B **36**, 7262 (1987).
[27] I. W. Chen, S. J. Keating, C. Y. Keating, X. Wu, J. Xu, P. E. Reyes-Morel, and T. Y. Tien, Solid State Commun. **63**, 997 (1987).
[28] S. I. Park, C. C. Tsuei, and K. N. Tu, Phys. Rev. B **36**, 2305 (1987).
[29] R. J. Cava, B. Batlogg, C. H. Chen, E. A. Rietman, S. M. Zahurak, and D. Werder, Phys. Rev. B **36**, 5719 (1987).
[30] B. A. Aleksashin, V. I. Voronin, S. V. Verkhovskiĭ, B. N. Goshchitskiĭ, S. A. Davydov, Yu. I. Zhdanov, E. A. Kar'kin, V. L. Kozhevnikov, A. V. Mirmel'shteĭn, M. V. Sadovskiĭ, V. V. Serikov, and S. M. Cheshnitskiĭ, Zh. Eksp. Teor. Fiz. **95**, 678 (1989) [Sov. Phys. JETP **68**, 382 (1989)].
[31] L. R. Testardi, W. G. Mouton, H. Mathias, H. K. Ng, C. M. Rey, and R. J. Kennady, Phys. Rev. B **36**, 8816 (1987).
[32] Yu. N. Shvachko, D. Z. Khusainon, A. A. Romanyukha, and V. V. Ustinov, Solid State Commun. **69**, 611 (1989).
[33] A. A. Koshta, Yu. N. Shvachko, A. A. Romanyukha, and V. V. Ustinov, Bull. Magn. Res. **12**, 65 (1990).
[34] A. A. Koshta, A. A. Romanyukha, Yu. N. Shvachko, N. A. Viglin, V. V. Ustinov, and S. V. Naumov, Sverkhprovodimost' (KIAE) **3**(5), 838 (1990) [Superconductivity **3**(5), 787 (1990)].
[35] D. K. De, J. Phys. C **21**, 4481 (1988).
[36] A. G. Maksimov, A. V. Dmitriev, L. V. Zolotukhina, V. S. Gorshkov, Ya. N. Blinovskov, and V. L. Kozhevnikov, Sverkhprovodimost' (KIAE) **2**, 39 (1989).
[37] N. E. Alekseevskiĭ, I. A. Garifullin, N. N. Garif'yanov, V. I. Kochelaev, A. V. Mitin, V. I. Nizhankovskiĭ, L. R. Tagirov, and E. P. Khlybov, Zh. Eksp. Teor. Fiz. **94**(4), 276 (1988) [Sov. Phys. JETP **67**, 805 (1988)].
[38] N. E. Alekseevskiĭ, I. A. Garifullin, N. N. Garif'yanov, B. I. Kochelaev, V. I. Nizhankovskiĭ, L. R. Tagirov, and E. P. Khlybov, Fiz. Tverd. Tela (Leningrad) **30**, 1568 (1988) [Sov. Phys. Solid State **30**, 909 (1988)].
[39] B. I. Kochelaev, N. E. Alekseevskiĭ, I. A. Garifullin, N. N. Garif'yanov, A. V. Mitin, V. I. Nizhankovskiĭ, L. R. Tagirov, G. G. Khaliullin, and E. P. Khlybov, Proc. 24th Ampere Congress, Poznan (1988), p. 429.
[40] N. E. Alekseevskiĭ, I. A. Garifullin, N. N. Garif'yanov, B. I. Kochelaev, A. V. Mitin, V. I. Nizhankovskiĭ, L. P. Tagirov, G. G. Khaliullin, and E. P. Khlybov, Pis'ma Zh. Eksp. Teor. Fiz. **48**, 36 (1988) [JETP Lett. **48**, 37 (1988)].
[41] G. Amoretti, E. Buluggiu, A. Vera, G. Galestani, and F. C. Matacotta, Z. Phys. B **72**, 17 (1988).
[42] K. N. Shrivastava, J. Phys. C **20**, L782 (1987).
[43] C. Rettori, D. Davidov, I. Belaish, and I. Felner, Phys. Rev. B **36**, 4028 (1987).
[44] J. Kohara, H. Yamagata, M. Matsumura, Y. Yamada, I. Nakada, E. Sakagumi, Y. Oda, and K. Asayama, Tech. Rep. ISSP Ser. A, No. 1835 (1987).
[45] D. L. Lyfar', S. M. Ryabchenko, A. A. Motuz, and D. R. Moiseev, Fiz. Nizk. Temp. **13**, 876 (1987). [Sov. J. Low Temp. Phys. **13**, 503 (1987)].
[46] K. Kojima, K. Ohbayashi, M. Udagawa, and T. Hihara, Jpn. J. Appl. Phys. **26**, L766 (1987).
[47] G. J. Bowden, P. R. Elliston, K. T. Wan, S. X. Don, K. E. Easterling, A. Bourdillou, C. C. Serrell, B. A. Cornel, and F. Separovic, J. Phys. C **20**, L545 (1987).
[48] J. De Aguiar, O. Albino, A. A. Menovsky, J. van den Berg, and H. B. Brom, Physica C **153–155**, 743 (1988).
[49] N. E. Alekseevskiĭ, A. V. Mitin, V. I. Nizhankovskiĭ, I. A. Garifullin, N. N. Garif'yanov, G. G. Khaliullin, E. P. Khlybov, B. I. Kochelaev, and L. R. Tagirov, J. Low Temp. Phys. 77, 87 (1989).
[50] A. Deville, B. Gaillard, H. Noel, M. Potel, P. Gougeon, and J. C. Levet, Physica C **153–155** 669 (1988).
[51] F. J. Owens, B. L. Ramakrishna, and Z. Iqbal, Physica C **156**, 221 (1988).
[52] E. W. Ong, B. L. Ramakrishna, and Z. Iqbal, Solid State Commun. **66**, 171 (1988).
[53] D. Shaltiel, J. Genossar, A. Graevsky, Z. H. Kalman, B. Fisher, and N. Kaplan, Solid State Commun. **63**, 987 (1987).
[54] F. Mehran, S. E. Barnes, T. R. McGuire, T. R. Dinger, D. L. Kaiser, and F. Holtzberg, Solid State Commun. **66**, 299 (1988).
[55] F. Mehran, S. E. Barnes, E. A. Guess, and T. R. McGuire, Solid State Commun. **67**, 55 (1988).
[56] J. De Aguiar, O. Albino, A. A. Menovsky, J. van den Berg, and N. B. Brom, J. Phys. C **21**, L237 (1988).
[57] A. A. Romanyukha, Yu. N. Shvachko, V. Yu. Irkhin, M. I. Katsnelson, A. A. Koshta, and V. V. Ustinov, Physica C **170**, 276 (1990).
[58] H. Kikuch, Y. Ajiro, Y. Ueda, K. Kosuge, M. Takano, Y. Takeda, and M. Sato, J. Phys. Soc. Jpn. **57**, 1887 (1988).
[59] R. N. Schwartz, R. C. Pastor, K. W. Kirby, and D. Rutz, Phys. Rev. B **36**, 8858 (1987).
[60] M. T. Causa, C. Fainstein, G. Nieva, R. Sanchez, L. R. Steren, M. Tovar, R. Zysler, D. C. Vier, S. Schultz, S. B. Oseroff, Z. Fisk, and J. L. Smith, Phys. Rev. B **38**, 257 (1988).
[61] F. Mehran, S. E. Barnes, C. C. Tsuei, and T. R. McGuire, Phys. Rev. B **36**, 7266 (1987).
[62] A. G. Badalyan, P. G. Baranov, V. I. Aleksandrov, M. A. Borik, and V. V. Osiko, Pis'ma Zh. Eksp. Teor. Fiz. **49**, 606 (1989) [JETP Lett. **49**, 697 (1989)].
[63] S. B. Oseroff, D. Rao, F. Wright, M. Tovar, D. C. Vier, S. Schultz, J. D. Thomson, K. Z. Fisk, and S.-W. Cheong, Solid State Commun. **70**, 1159 (1989).
[64] S. B. Oseroff, D. C. Vier, J. F. Smyth, C. T. Salling, S. Schultz, Y. Delichaouch, B. W. Lee, M. B. Lee, M. B. Maple, Z. Fisk, J. D. Thompson, J. L. Smith, and E. Zirngiebl, Solid State Commun. **64**, 241 (1987).
[65] G. Galestani, G. Rizzoli, G. D. Andretti, E. Buluggiu, D. C. Giori, A. Valenti, A. Vera, and G. Amoretti, Physica C **158**, 217 (1989).
[66] F. J. Dyson, Phys. Rev. **98**, 349 (1955).
[67] T. Kobayashi, H. Katsuda, K. Hayashi, M. Tokumoto, and H. Ihara, Jpn. J. Appl. Phys. **27**, L670 (1988).
[68] A. A. Gippius, V. V. Moshchalkov, Yu. A. Koksharov, A. N. Tikhonov, B. V. Mill, and Y. Zoubkova, Mod. Phys. Lett. Ser. B **3**, 427 (1989).
[69] P. Burlet, C. Vettier, M. J. G. M. Jurgens, J. Y. Henry, J. Rossat-Mignod, H. Noel, M. Pote, P. Gougen, and J. C. Levet, Physica C **153–155**, 1115 (1988).
[70] J. M. Tranguada, D. E. Cox, W. Kunnmann, H. Mouden, G. Shirane, M. Suenaga, P. Zolliker, D. Vaknin, S. K. Sinha, M. S. Alvarez, A. J. Jacobson, and D. C. Johnston, Phys. Rev. Lett. **60**, 156 (1988).
[71] D. Shaltiel, H. Bill, P. Fischer, M. Francois, H. Hagemann, M. Peter, Y. Ravisekhar, W. Sadowsky, H. J. Scheel, G. Triscone, E. Walker, and K. Yvon, Physica C **158**, 424 (1989).
[72] A. Janossy, A. Rockenbauer, and S. Pekker, Physica C **167**, 301 (1990).
[73] R. Beyers, G. Lim, E. M. Engler, V. Y. Lee, M. L. Ramirez, R. J. Savoy, R. D. Jacowitz, T. M. Shaw, S. La Placa, R. Boehme, C. C. Tsuei, Park Sung I, M. W. Shafer, and W. J. Gallagher, Appl. Phys. Lett. **51**, 614 (1987).
[74] R. L. Cava, B. Batlogg, S. A. Sunshine, T. Siegrist, R. M. Fleming, K. Rabe, L. F. Schneemeyer, D. W. Murphy, R. B. van Dover, P. K. Gallagher, S. H. Glarum, S. Nakahara, R. C. Farrow, J. J. Krajewski, S. M. Zahurak, J. V. Waszczak, J. H. Marshall, P. Marsh, L. W. Rupp Jr., W. F. Peck, and E. A. Rietman, Physica C **153–155**, 560 (1988).
[75] R. L. Cava, B. Batlogg, K. M. Rabe, E. A. Rietman, P. K. Gallagher, and L. W. Rupp, Physica C **156**, 523 (1988).
[76] B. D. Dunlap, J. D. Jorgensen, C. Serge, A. E. Dwight, J. L. Matykiewicz, H. Lee, W. Peng, and C. W. Kimbol, Physica C **158**, 571 (1989).
[77] L. N. Bulaevskiĭ, F. V. Zvarykina, Yu. S. Karimov, R. B. Lyubovskiĭ, and I. F. Shchegolev, Zh. Eksp. Teor. Fiz. **62**, 725 (1972) [Sov. Phys. JETP **35**, 384 (1972)].
[78] Yu. N. Shvachko, A. A. Romanyukha, A. V. Skripov, and V. V. Ustinov, Bull. Magn. Res. **12**, 62 (1990).
[79] A. Abragam and B. Bleaney, *Electron Paramagnetic Resonance of Transition Ions*, Clarendon Press, Oxford, 1970 [Russ. transl., Vol. 1, Mir, M., 1972].
[80] D. Shaltiel, S. E. Barnes, H. Bill, M. Francois, H. Hagemann, J. Jegondaz, D. Lovy, P. Monod, M. Peter, A. Revsolevschi, W. Sadowski, and E. Walker, Physica C **161**, 13 (1989).
[81] H. Szymczak, R. Zuberek, and A. Pajaczkowska, J. Phys. F **18**, 1889 (1988).
[82] S. K. Misra and L. E. Misiak, Solid State Commun. **72**, 351 (1989).
[83] A. G. Vedeshwar, Md. Shahbuddin, Prem Chand, H. D. Bist, S. K. Agarwal, V. N. Moorthy, C. V. N. Rao, and A. V. Narlikar, Physica C **158**, 385 (1989).
[84] P. Regnier, R. P. Gupta, and P. Truchot, J. Phys. C **21**, L463 (1988).
[85] B. Jayaram, S. K. Agarwal, K. C. Nagpal, A. Gupta, and A. V. Narliker, Magn. Res. Bull. **23**, 701 (1988).
[86] Abdulsabirov, R. Shch. Zhdanov, Ya. S. Izygson, S. L. Korableva, I. N. Kurkin, L. L. Sedov, I. V. Yasonov, and B. Lippol'd, Sverkhprovodimost' (KIAE) **2**, 52 (1989).
[87] Ya. N. Blinovskov, I. A. Leonidov, and I. L. Kozhevnikov, Fiz. Met. Metalloved. **64**, 338 (1987). [Phys. Met. Metallogr. USSR **64**, 119 (1987)].
[88] V. E. Kataev, E. F. Kukovitskiĭ, G. B. Teĭtel'baum, and A. M. Finkel'shteĭn, Pis'ma Zh. Eksp. Teor. Fiz. **51**, 115 (1990). [JETP Lett. **51**, 129 (1990)].
[89] J. De Aguiar, O. Albino, J. van der Berg, H. B. Brom, Nieuwenhuys, J. A. Mydosh, F. P. F. van Berkel, and H. W. Zandbergen, Physica C **156**,

571 (1988).
[90] N. Moser, A. Hofmann, P. Schule, R. Henes, and H. Kronmuller, Z. Phys. B **71**, 37 (1988).
[91] P. Vasek, L. Smroka, J. Dominec, M. Resek, O. Smrckova, and D. Sykova, Solid State Commun. **69**, 23 (1989).
[92] M. D. Sastry, C. Natarajan, A. G. I. Dalvi, and R. M. Iyer, Physica C **160**, 69 (1989).
[93] B. Rakvin, M. Pozek, and A. Dulcic, Solid State Commun. **72**, 199 (1989).
[94] Yu. N. Shvachko, A. A. Koshta, A. A. Romanyukha, V. V. Ustinov, and A. I. Akimov, Physica C **173**, 350 (1991).
[95] P. Pincus, A. C. Gossard, V. Jaccarino, and J. H. Wernick, Phys. Lett. **13**, 21 (1964).
[96] D. R. Harshman, L. F. Schneemeyer, J. V. Waszczak, G. Aeppli, R. J. Cava, B. Batlogg, L. W. Rupp, E. J. Ansalmo, and D. Ll. Williams, Phys. Rev. B **39**, 851 (1989).
[97] H. Niki, T. Suzuki, S. Tomiyoshi, H. Hentona, M. Omori, T. Kajitani, T. Kamiyama, and R. Igei, Solid State Commun. **69**, 547 (1989).
[98] E. F. Kukovitskiĭ, S. G. L'vov, Yu. N. Talanov, G. B. Teĭtel'baum, and V. A. Shustov, Pis'ma Zh. Eksp. Teor. Fiz. **51**, 61 (1990) [JETP Lett. **51**, 73 (1990)].
[99] J. Stankowski, P. K. Kahol, N. S. Dalal, and J. S. Moodera, Phys. Rev. B **36**, 7126 (1987).
[100] R. Durny, J. Hautala, S. Ducharme, B. Lee, O. C. Symko, P. C. Taylor, D. J. Zheng, and J. A. Xu, Phys. Rev. B **36**, 2361 (1987).
[101] M. D. Sastry, A. G. I. Dalvi, Y. Babu, R. M. Kadam, J. V. Yakhmi, and K. M. Iyer, *Nature* **330**, 49 (1987).
[102] K. Khachaturyan, E. R. Weber, P. Tejedor, A. M. Stacy, and A. M. Portis, Phys. Rev. B **36**, 8309 (1987).
[103] K. W. Blazey, K. A. Müller, J. G. Bednorz, W. Berlinger, G. Amoretti, E. Bullugiu, A. Vera, and F. C. Mattacotta, Phys. Rev. B **36**, 7241 (1987).
[104] M. D. Sastry, Y. Babu, R. M. Kadam, A. G. I. Dalvi, I. K. Gopalakrishnan, J. V. Yakhmi, and R. M. Iyer, J. Phys. C **21**, L607 (1988).
[105] S. V. Bhat, P. Gangulu, T. V. Ramakrishnan, and C. N. R. Rao, J. Phys. C **20**, L559 (1988).
[106] V. F. Masterov, A. I. Egorov, N. P. Gerasimov, S. V. Kozyrev, I. L. Likholit, I. G. Savel'ev, A. V. Fedorov, and K. F. Shtel'makh, Pis'ma Zh. Eksp. Teor. Fiz. **46**, 289 (1987) [JETP Lett. **46**, 364 (1987)].
[107] R. S. Liu, Jpn. J. Appl. Phys. **28**, L2175 (1989).
[108] K. W. Blazey and I. Mangelschots, Physica C **170**, 267 (1990).
[109] S. B. Oseroff, D. Rao, F. Wright, D. C. Vier, S. Schultz, J. D. Thompson, Z. Fisk, S.-W. Cheong, M. F. Hundley, and M. Tovar, Phys. Rev. B **41**, 1934 (1990).
[110] M. D. Sastry, K. S. Ajayakumar, R. M. Kadam, G. M. Phatak, and R. M. Iyer, Physica C **170**, 41 (1990).
[111] A. C. Bodi, Phys. Rev. B **41**, 2127 (1990).
[112] M. Pozek, A. Dulcic, and B. Rakvin, Solid State Commun. **70**, 889 (1989).
[113] A. Dulcic, B. Leontic, M. Peric, and B. Rakvin, Europhys. Lett. **4**, 1403 (1987).
[114] M. Pozek, A. Dulcic, and B. Rakvin, "Field-modulated microwave absorption in granular superconductors: first and second harmonic signal," University of Zagreb preprint (1990).
[115] A. Dulcic, B. Rakvin, and M. Pozek, "Mechanisms of field dependence microwave absorption in high-T_c ceramic superconductors," University of Zagreb preprint (1990).
[116] M. Peric, B. Rakvin, M. Prester, N. Brnicevic, and A. Dulcic, Phys. Rev. B **37**, 522 (1988).
[117] K. W. Blazey, A. M. Portis, and J. G. Bednorz, Solid State Commun. **65**, 1153 (1988).
[118] K. W. Blazey, A. M. Portis, K. A. Müller, J. G. Bednorz, and F. H. Holtzberg, Physica C **153–155**, 56 (1988).
[119] A. M. Portis, *Proceedings of International School of Materials Science and Technology* (ed. by K. A. Müller and J. G. Bednorz), Springer Verlag, Berlin, 1989, p. 24.
[120] K. W. Blazey, A. M. Portis, K. A. Müller, and F. H. Holtzberg, Europhys. Lett. **6**, 457 (1988).
[121] K. W. Blazey, A. M. Portis, and F. H. Holtzberg, Physica C **157**, 16 (1989).
[122] K. W. Blazey and F. H. Holtzberg, IBM J. Res. Dev. **33**, 324 (1989).
[123] E. V. Gal'tseva, A. A. Dubinskiĭ, V. A. Zhorin, G. G. Lazarev, and Ya. S. Lebedev, Sverkhprovodimost' (KIAE) **2**(10), 62 (1989) [*Superconductivity* **2**(10), 70 (1989)].
[124] A. S. Kheĭfets, A. I. Veĭnger, and S. V. Kozakov, Sverkhprovodimost' (KIAE) **2**(10), 69 (1989) [Superconductivity **2**(10), 78 (1989)].
[125] A. S. Kheifets and A. I. Veinger, Physica C **165**, 491 (1990).
[126] F. J. Owens and Z. Iqbal, Physica C **171**, 238 (1990).
[127] R. Karim, R. Seed, S. A. Oliver, A. Widom, and C. Vittoria, IEEE Trans. Magn. **MAG-25**, 3221 (1989).
[128] A. Gould, S. D. Tyagi, S. W. Bhagat, and M. A. Manheimer, IEEE Trans. Magn. **MAG-25**, 3224 (1989).
[129] I. Ciccarello, C. Fazio, M. Guccione, and M. Li Vigni, Physica C **159**, 769 (1989).
[130] S. N. Smirnov, *Sverkhprovodimost'* (KIAE), 11 (1989).
[131] C. Ebner and D. Stroud, Europhys. Lett. **6**, 457 (1988).
[132] A. A. Abrikosov, *Fundamentals of the Theory of Metals*, North-Holland, Amsterdam, 1988 [Russ. original, Nauka, Moscow, 1987].
[133] E. B. Sonin and A. K. Tagantsev, Zh. Eksp. Teor. Fiz. **95**, 994 (1989) [Sov. Phys. JETP **68**, 572 (1989)].
[134] E. B. Sonin, Pis'ma Zh. Eksp. Teor. Fiz. **47**, 415 (1988) [JETP Lett. **47**, 496 (1988)].
[135] A. R. Strnad, C. F. Hempstead, and Y. B. Kim, Phys. Rev. Lett. **13**, 794 (1964).
[136] S. W. Tozer, A. W. Kleinsasser, T. Penney, D. L. Kaizer, and F. H. Holtzberg, Phys. Rev. Lett. **59**, 1768 (1987).
[137] A. Umezawa, G. W. Crabtree, J. Z. Liu, T. J. Moran, S. K. Malik, L. N. Nunez, W. L. Kwok, and C. H. Sowers, Phys. Rev. B **38**, 2843 (1988).
[138] W. J. Gallagher, T. K. Worthington, T. R. Dinger, F. H. Holtzberg, D. L. Kaizer, and R. L. Sandstrom, Physica B **148**, 228 (1987).
[139] J. T. Suss, W. Berlinger, A. M. Portis, and K. A. Müller, Solid State Commun. **71**, 929 (1989).
[140] G. G. Siu, Solid State Commun. **72**, 291 (1989).
[141] A. Dulcic, R. H. Crepeau, and J. H. Freed, Phys. Rev. B **38**, 5002 (1988).
[142] L. F. Schneemeyer, J. K. Thomas, T. Siegrist, B. Batlogg, L. N. Rupp, R. L. Opila, R. J. Cava, and D. W. Murphy, *Nature* **38**, 601 (1987).
[143] Yu. N. Shvachko, A. A. Romanyukha, A. P. Stepanov, V. L. Kozhevnikov, and S. M. Cheshnitskiĭ, Fiz. Met. Metalloved. **94**, No. 2, 401 (1988). [Phys. Met. Metallogr. (USSR) **94**, 180 (1988)].
[144] A. I. Tsapin, Dokl. Akad. Nauk SSSR **295**, 1112 (1987) [Sov. Phys. Dokl. **32**, 673 (1987)].
[145] M. Cardona, J. Gittleman, and B. Rosenblum, Phys. Lett. **17**, 92 (1965).
[146] C. P. Bean, Rev. Mod. Phys. **36**, 31 (1964).
[147] M. Tinkham, *Introduction to Superconductivity*, McGraw-Hill, N.Y., 1975 [Russ. transl., Atomizdat, M., 1980].

Translated by Steve Torstveit